12-2008

# Hydrogen Production Using Geothermal Energy

Theodore Wayne Hand
*Utah State University*

# HYDROGEN PRODUCTION USING GEOTHERMAL ENERGY

by

Theodore W. Hand

A thesis submitted in partial fulfillment
of the requirements for the degree

of

MASTER OF SCIENCE

in

Mechanical Engineering

Approved:

| | |
|---|---|
| Dr. Byard Wood<br>Major Professor | Dr Stephen Whitmore<br>Committee Member |
| Dr. Heng Ban<br>Committee Member | Dr. Byron R. Burnham<br>Dean of Graduate Studies |

UTAH STATE UNIVERSITY
Logan, Utah

2008

## Abstract

Hydrogen Production Using Geothermal Energy

by

Theodore W. Hand, Master of Science

Utah State University, 2008

Major Professor: Dr. Byard Wood
Department: Mechanical and Aerospace Engineering

With an ever-increasing need to find alternative fuels to curb the use of oil in the world, many sources have been identified as alternative fuels. One of these sources is hydrogen. Hydrogen can be produced through an electro-chemical process. The objective of this report is to model an electrochemical process and determine gains and or losses in efficiency of the process by increasing or decreasing the temperature of the feed water. In order to make the process environmentally conscience, electricity from a geothermal plant will be used to power the electrolyzer. Using the renewable energy makes the process of producing hydrogen carbon free. Water considerations and a model of a geothermal plant were incorporated to achieve the objectives.

The data show that there are optimal operating characteristics for electrolyzers. There is a 17% increase in efficiency by increasing the temperature from 20ºC to 80ºC. The greater the temperature the higher the efficiencies, but there are trade-offs with the required currents.

(94 pages)

## Acknowledgments

The author gratefully acknowledges the financial support of Derek Morse and the Regional Transportation Commission of Washoe County, Nevada.

Those family members, friends, my advisor, and committee who have helped motivate me to this point.

Theodore W. Hand

Contents

## List of Tables

## List of Figures

## Nomenclature

| | |
|---|---|
| $A$ | Area of electrodes |
| $a_1$ | Faraday efficiency |
| $C_T$ | overall thermal capacity |
| $F$ | Faraday's constant |
| $I_{density}$ | Current density [mA / $cm^2$] |
| $I_{ely}$ | Electrical current (ely load) [A] |
| $n$ | number of electrons transferred |
| $\eta_e$ | Energy efficiency |
| $\eta_f$ | Faraday efficiency |
| $\eta_{tot}$ | Overall efficiency |
| $R_T$ | electrolyzer resistance |
| $r_1$ | Ohmic resistance [$\Omega\ m^2$] |
| $R_2$ | Ohmic resistance [$\Omega\ m^2/°C$] |
| $s_1$ | Overvoltage on electrodes [V] |
| $T_{ely}$ | Ely operating temperature [°C] |
| $t_1$ | Overvoltage on electrodes [$m^2/A$] |
| $t_2$ | Overvoltage on electrodes [$m^2°C/A$] |
| $t_3$ | Overvoltage on electrodes [$m^2°C/A$] |
| $U_{cell}$ | Cell voltage (per cell) [V] |
| $U_{rev}$ | Reversible voltage (per cell) [V] |
| $U_{tn}$ | Thermoneutral cell voltage [V] |

# Chapter 1

# INTRODUCTION AND PROBLEM STATEMENT

## 1.1 Introduction

Hydrogen is one of the fuels that has been suggested to help reduce the use of fossil fuels in the United States. Today approximately 9 billion kilograms of hydrogen are produced annually [1]. More than 95% of the merchant hydrogen is used for industrial applications in the chemical, metals, electronics, and space industries. There are several methods used to produce hydrogen. These methods include: natural gas reforming, electrolysis, liquid reforming, nuclear high-temperature electrolysis, high-temperature thermo-chemical water-splitting, photo-biological, and photo-electrochemical. Steam methane reforming accounts for 80% of the hydrogen produced. The remaining 20% is a by-product of chemical processes such as chlor-alkali production. Water electrolysis represents only a niche segment of the merchant hydrogen market [2].

Electrolysis is the process of making a non-spontaneous process occurs by applying an external power supply to the application [3]. A number of existing and planned demonstration projects are using or will use electrolysis, even though it is one of the more energy intensive processes for producing hydrogen. However, it provides a pathway for producing hydrogen from carbon free renewable energy.

Competitive energy costs, reliability of a system and ease of use are the three major factors which determine whether a proposed system is worth implementing. The increased availability of cleaner and inexhaustible energy sources allows a user to seriously consider renewable sources. Stand-alone residential systems utilizing

renewable energy are also attracting increasing interest. This attention is perhaps related to lowered renewable energy costs, increased reliability and desire to be in control of one's energy future. Of the available fuel sources today, hydrogen is suited to become a driving force in each and every energy scenario. This is mainly because hydrogen as a fuel produces high amounts of energy without any relative pollution. Recently, extensive research has explored the methods which can be used to produce hydrogen efficiently.

These methods and others are currently undergoing research with the goal of increasing efficiencies, quality, and quantities economically. Currently, there are a number of hydrogen fuel demonstration projects to evaluate efficiency. This thesis research was developed to support a research project being carried out by the Washoe County, Nevada, Regional Transportation Commission (RTC).

## 1.2 RTC Hydrogen Project - $H_2$Fuel

Washoe County, Nevada, Regional Transportation Commission (RTC) has initiated a hydrogen fuel project named: *$H_2$Fuel: The Production, Storage, Distribution, and Use of Hydrogen Fuel by Transit Systems* [4].

$H_2$Fuel is an integrated, geothermal powered, hydrogen-fuel production and use cycle with robust characteristics suited to real world mass transit conditions. It is literally a "well to wheels" research project. Hydrogen fuel is produced using 100% carbon free renewable energy.

$H_2$Fuel includes a geothermal electrical generation facility to power a hydrogen-fuel production facility utilizing electrolysis. This project includes facilities for hydrogen storage, transmission, distribution, dispensing fuel, maintaining hydrogen-powered vehicles, and for personnel training for all aspects of hydrogen production and utilization.

A number of transit vehicles using various types of hydrogen-powered propulsion systems will be operated, using the supplied fuel, and maintained under real world conditions. $H_2$Fuel builds upon RTC's successful experience using CNG-powered vehicles for its CitiLift service (Paratransit Vehicles).

$H_2$Fuel is a nine-year, multi-step transition from diesel fuel to hydrogen fuel for RTC's fixed-route bus fleet (Citifare). Each step represents a major transition milestone. A blended-fuel mixture of hydrogen and compressed natural gas (HCNG) is well established and will be used in the first phase. Hybrid-electric vehicles powered by hydrogen-fueled internal combustion engines will be the second phase. The final phase will involve the introduction of fuel cell powered buses.

Table 1.1: $H_2$fuel Transition Strategy Summary

| YEAR | TRANSITION STEP | H2 REQUIRED kg/day | H2 PRODUCTION COSTS | | Power Required* kW | Water Required Gal/day | Equipment Space Required $Ft^2$ |
|---|---|---|---|---|---|---|---|
| | | | EQUIPMENT $1000 | ELECTRICITY $/day @ $0.10/kwh | | | |
| 2006 | 10 HCNG Paratransit Vehicles | 13.0 | 51 - 63 | 83 | 34 | 55 | 300 |
| 2007 | 20 HCNG Paratransit Vehicles | 26.0 | 51 – 63 | 165 | 69 | 110 | 300 |
| 2008 | 30 HCNG Paratransit | 39.0 | 211 - 260 | 248 | 103 | 165 | 300 |
| 2009 | 35 HCNG Paratransit<br>5 H2 ICE Hybrid Paratransit vehicles | 78.0 | 160 - 197 | 454 | 189 | 302 | 600 |
| 2010 | 30 HCNG Paratransit<br>10 H2 ICE Hybrid Paratransit<br>5 H2 ICE Powered Bus (40 ft) vehicles | 314.0 | 1,042 – 1,286 | 1,993 | 830 | 1,328 | 2,500 |
| 2011 | 30 HCNG Paratransit<br>10 H2 ICE Hybrid Paratransit<br>10 H2 ICE Powered Bus (40 ft) vehicles | 524.0 | 1,042 – 1,286 | 3,326 | 1,386 | 2,217 | 5,000 |
| 2012 | 30 HCNG Paratransit<br>10 H2 ICE Hybrid Paratransit<br>5 H2 ICE Powered Bus (40 ft) vehicles<br>5 H2 Fuel Cell Powered Buses (40 ft) | 524.0 | 0 | 3,326 | 1,386 | 2,217 | 5,000 |
| 2013 | 30 HCNG Paratransit<br>10 H2 ICE Hybrid Paratransit<br>5 H2 ICE Powered Bus (40 ft) vehicles<br>5 H2 Fuel Cell Powered Buses (40 ft) | 524.0 | 0 | 3,326 | 1,386 | 2,217 | 5,000 |
| 2014 | 30 HCNG Paratransit<br>10 H2 ICE Hybrid Paratransit<br>5 H2 ICE Powered Bus (40 ft) vehicles<br>5 H2 Fuel Cell Powered Buses (40 ft) | 524.0 | 0 | 3,326 | 1,386 | 2,217 | 5,000 |

* The power required assumes compressed gas storage and no hydrogen liquefaction.

This transition strategy allows for the gradual training of RTC in handling fuel tanks and fueling systems that consist of compressed hydrogen gas, as well as becoming comfortable with hydrogen as a safe alternative fuel. Figure 1.1 summarizes $H_2$Fuel's strategy.

## 1.3 Proposed Research and Scope of Work

The nature of this project is to develop a system simulation model for a hydrogen production system consisting of a geothermal power plant, an electrolyzer, and hydrogen storage. Electrolysis is one of the more energy extensive processes; however, when coupled with a carbon-free electricity production facility this process becomes more attractive. This research also models an electrochemical process and determines gains and or losses in efficiency of the process by increasing or decreasing the temperature of the feed water.

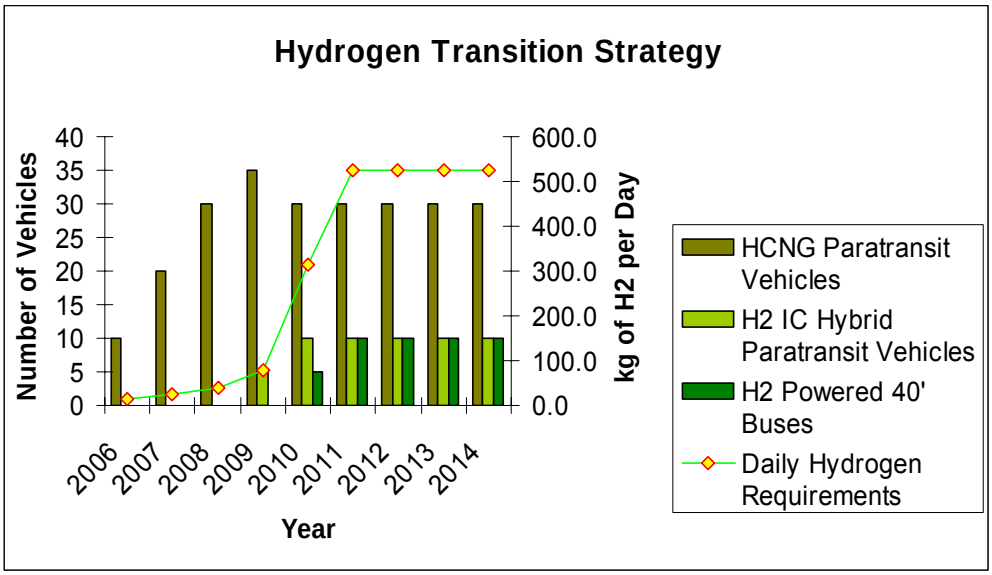


Fig. 1.1: $H_2$Fuel vehicle acquisition and hydrogen production schedules.

To achieve the objectives of the proposed research, a TRaNsient System Simulation program (TRNSYS) was used for modeling purposes. TRNSYS is a simulation environment for the transient simulation of energy systems. It is used to validate and design new energy concepts, their equipment, control strategies, occupant behavior, alternative energy systems, etc. An open, modular structure that allows the user to access the source code and manipulate that code as the user sees fit [5]. The TRNSYS library [6-8] includes many of the components commonly found in thermal and electrical energy systems. It also includes component routines to handle input of weather data or other time-dependent forcing functions and output of simulation results. These components will be used to model the production of hydrogen.

After development, the model will be evaluated and strategies will be employed to increase the overall system efficiency. Geothermal heat will precondition the feed water for the electrolyzer, thereby making the overall process more competitive in the current energy market.

# Chapter 2

# BACKGROUND AND LITERATURE REVIEW

## 2.1 Current Status of Energy Sources

There are many sources of energy in the world today. All the comforts we enjoy today have been provided or are being provided by some from of energy. The energy is created from various resources provided by the earth. Our shelters, buildings, transportation, electricity, food, and clothing are provided by these resources. The main sources of energy are from coal, natural gas, crude oil, nuclear sources, and various forms of renewable energies. Coal, crude oil, and natural gas are classified as fossil fuels. As the population of the world increases and underdeveloped countries become developed, the need for fossil fuels grows.

Coal extracted from the ground by underground mining or open-pit mining (surface mining) is a readily combustible black or brownish-black sedimentary rock. It is composed primarily of carbon and other assorted other elements, including sulfur. Coal remains an enormously important fuel. It is the largest single source of fuel for the generation of electricity world-wide. When coal is used for electricity generation, it has a thermodynamic efficiency of about 35–40% for the entire process. Approximately 40% of the world electricity production uses coal, and the total known deposits recoverable by current technologies are sufficient for 300 years' use at current rates [9].

Natural gas is a gaseous fossil fuel found in oil fields and natural gas fields, and in coal beds. The primary component of natural gas is methane ($CH_4$), the shortest and lightest hydrocarbon molecule. It also contains heavier gaseous hydrocarbons such as

ethane ($C_2H_6$), propane ($C_3H_8$), and butane ($C_4H_{10}$), as well as other sulfur containing gases, in varying amounts.

Additionally, natural gas also contains and is the primary market source of helium. Combustion of one cubic meter of commercial quality natural gas yields 39 mega-joules (10.6 kWh) of helium. Natural gas is also a major source for electricity generation. Particularly high efficiencies can be achieved through combining gas turbines with a steam turbine in a combined cycle mode. Combined cycle power generation using natural gas is therefore the cleanest source of power available using fossil fuels. Natural gas is also supplied to homes, where it is used for such purposes as cooking,

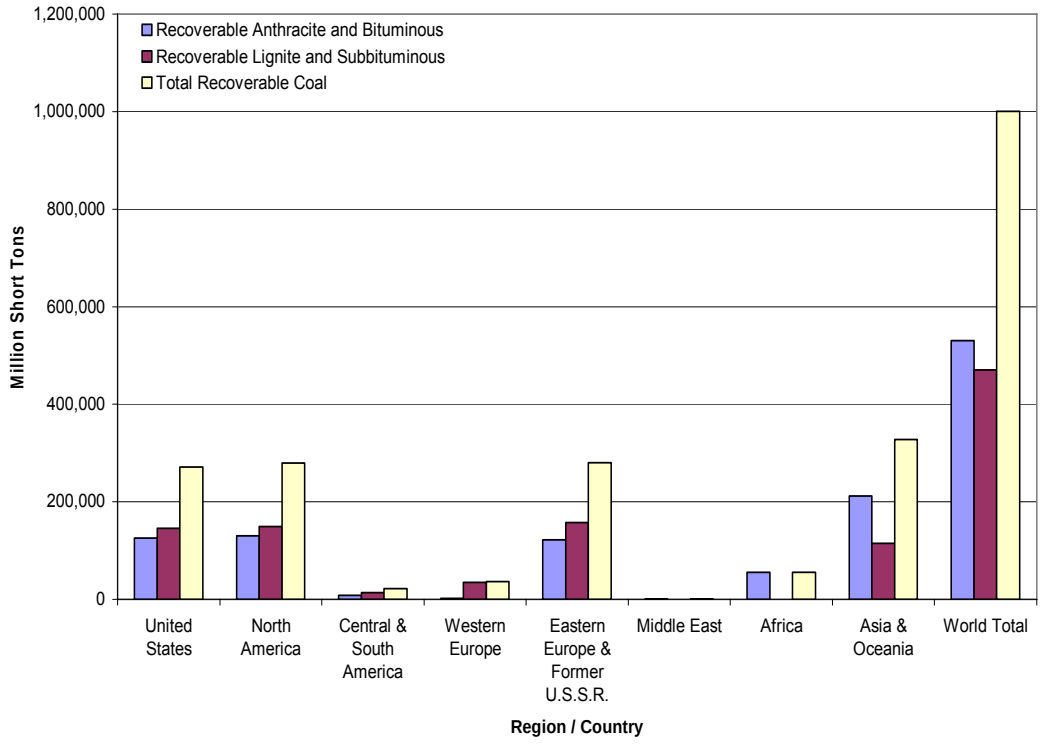


Fig. 2.1: World estimated recoverable coal [million short tons].

heating/cooling, and other utilities. Heating systems may include boilers, furnaces, and water heaters. Compressed natural gas (CNG) is used in rural homes without connections to piped-in public utility services, and in portable tanks such as those used in barbeque grills.

Natural gas also burns cleaner than other fossil fuels, such as oil and coal, and produces less greenhouse gas per unit energy released. For an equivalent amount of heat, burning natural gas produces about 30% less carbon dioxide than burning petroleum and about 45% less than burning coal [10]. This technology is widely used wherever gas can be obtained at a reasonable cost. Fuel cell technology may eventually provide even cleaner options for converting natural gas into electricity, but as yet it is not price-competitive.

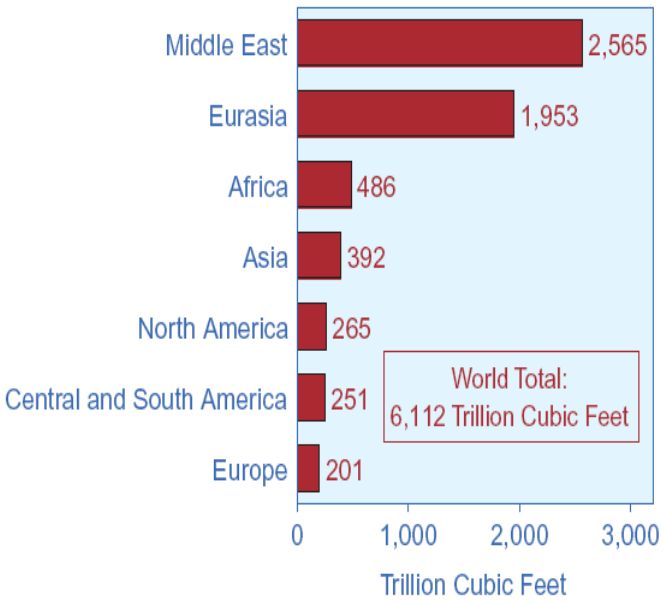


Fig. 2.2: World natural gas reserves as of Jan. 2006.

Crude Oil is a black, dark brown or greenish liquid found in the porous rock formations in the earth. The American Petroleum Institute, in its Manual of Petroleum Measurement Standards (MPMS), defines it as "a substance, generally liquid, occurring naturally in the earth and composed mainly of mixtures of chemical compounds of carbon and hydrogen with or without other nonmetallic elements such as sulfur, oxygen, and nitrogen."

It consists of a complex mixture of hydrocarbons, mostly alkenes, but may vary greatly in its appearance and composition. Petroleum is used mostly, by volume, for producing fuel oil and petrol (gasoline), both of which are important "primary energy" sources. Petroleum is also the raw material for many chemical products, including solvents, fertilizers, pesticides, and plastics. Around 84% (37 of 44 gallons in a typical barrel) of all petroleum extracted is processed as fuels, including gasoline, diesel, jet fuel, heating, and other fuel oils, and liquefied petroleum gas. The other 16% is converted into other materials such as plastic. Since petroleum is a non-renewable resource, there has always existed a concern of depletion of the resource in the near future [11]. Figure 2.4 displays the proven reserves of different areas throughout the world. Figures 2.5 – 2.6 summarize the energy consumption for various energy resources.

Total primary energy consumption, including energy for electricity generation, is predicted to grow by 1.1% per year from 2004 to 2030 (Fig. 2.5). Fossil fuels account for 88% of the growth, with coal use increasing by 53%, petroleum use increasing by 34%, and natural gas use increasing by 20% over that period. The increase in coal consumption occurs primarily in the electric power sector. This is due to a strong growth in electricity demand and favorable economics prompting an increase in the coal-fired base load

capacity. More than one-half of the increase in coal consumption is expected after 2020, when higher natural gas prices will make coal the fuel choice for future power plants.

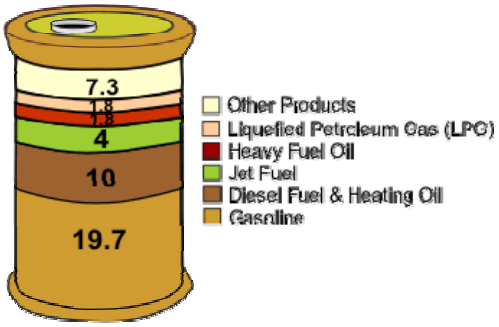


Fig. 2.3: Distribution of a 42 gallon barrel of crude oil.[1]

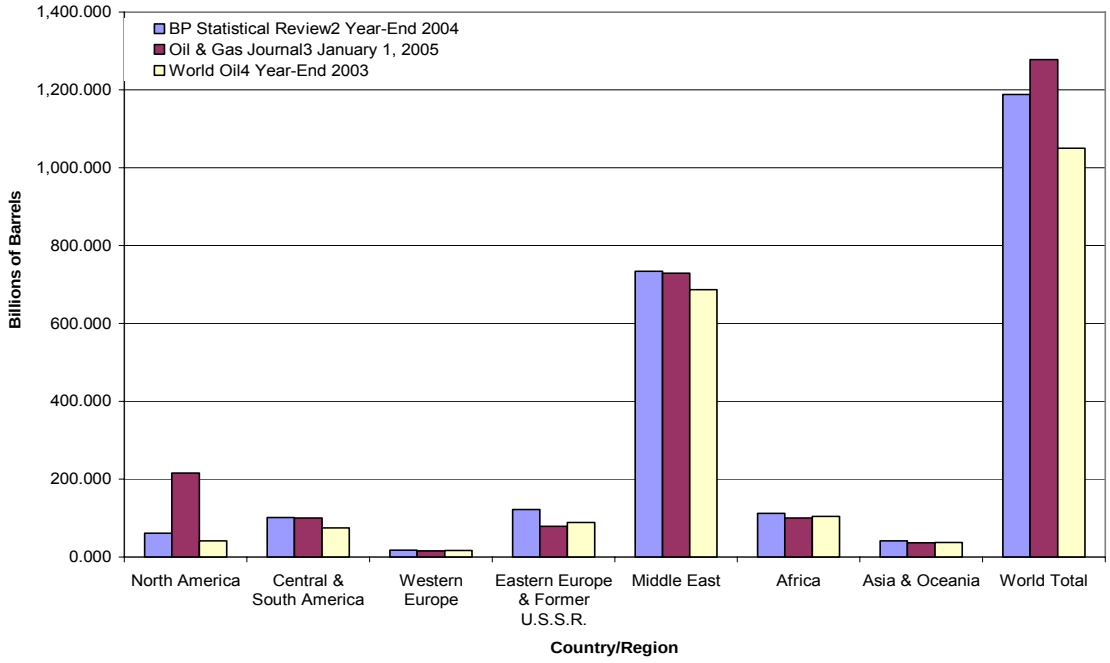


Fig. 2.4: World Proven Reserves of Oil.

[1] Note: A 42 U.S. gallon barrel of crude oil yields slightly more than 44 gallons of petroleum products. This "process gain" in volume is due to a reduction in density during the refining process.

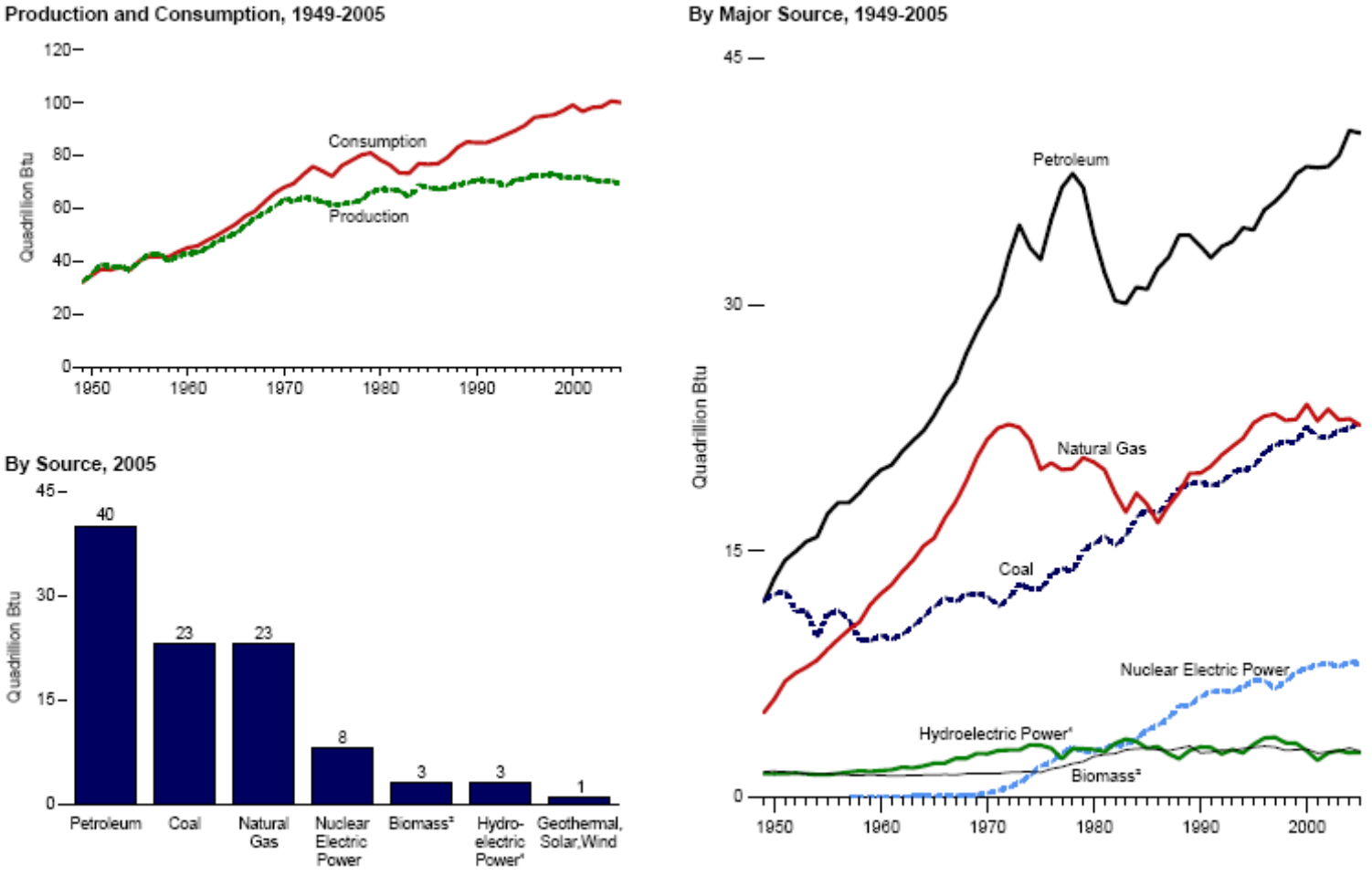


¹ Conventional hydroelectric power.
² Wood, waste, and alcohol fuels (ethanol blended into motor gasoline).

Note: Because vertical scales differ, graphs should not be compared.
Sources: Tables 1.2 and 1.3.

Fig. 2.5: Energy consumption by source.

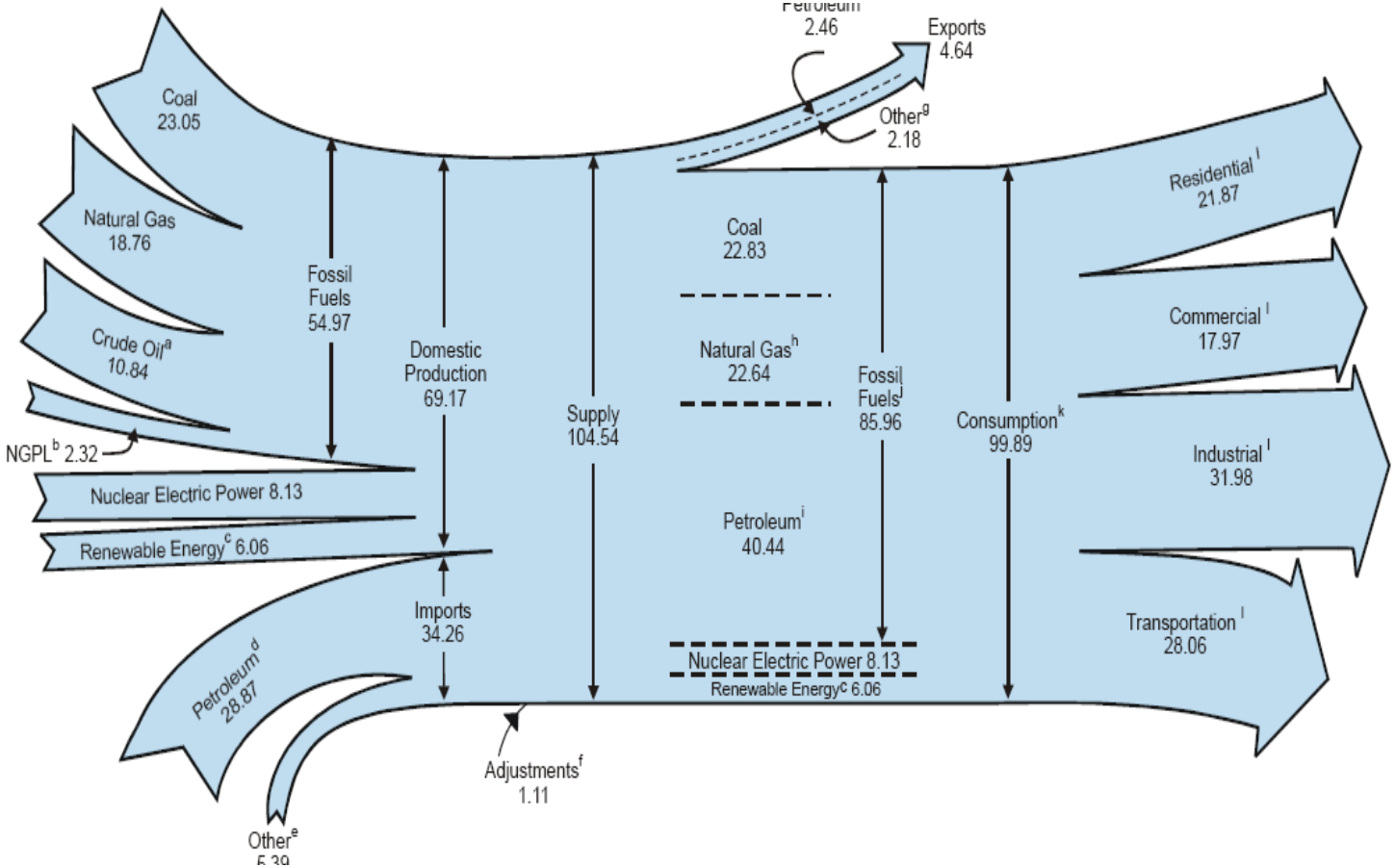


Fig. 2.6: Energy consumption by sector.

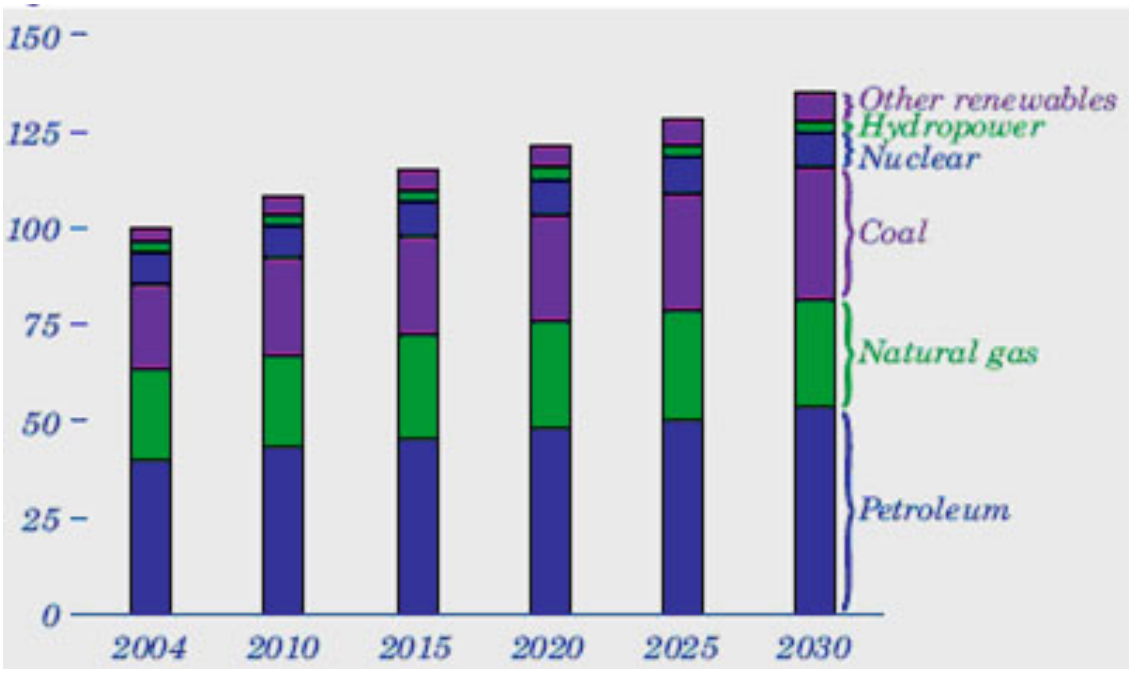


Fig. 2.7: Primary energy uses by fuel 2004-2030 [quadrillion Btu].

Growth in natural gas consumption for power generation is restrained by its high price relative to coal. Industry and buildings account for 71% of the increase in natural gas consumption from 2004 to 2030. Transportation accounts for 87% of the increase in petroleum consumption, dominated by growth in fuel use for light-duty vehicles. Fuel use by freight trucks, which is second in energy use among travel modes, grows by 1.9% per year on average. This is the fastest growing annual rate among the major forms of transportation. Petroleum use in the building sector, mostly for space heating, declines slightly in the projection. Renewable energy projects and rapid growth in energy production from non-hydroelectric renewable sources is partly a result of State mandates for renewable electricity generation and renewable energy production tax credits. An increase in power generation from nuclear energy is also projected, as tax credits spur construction of new nuclear plants in the future [9].

## 2.2 Hydrogen as a Fuel Source

Finding a sustainable energy source for the future is one of the more urgent tasks of today. With the exhaustion of fossil fuels, the energy economy will have to change from a chemical base to an electrical base. Further action needs to be taken in order to make this transition smooth. This will take years of research in order to provide viable sources of energy. In today's market a low cost energy source is sought after to provide an alternative to fossil fuels. Current energy sources are would be fossil fuels, nuclear fuels, natural gases, hydrogen fuels, sunlight, wind, fuel cells, and hybrid systems.

Hydrogen is one of the fuels suggested to help reduce the use of fossil fuels in the United States. Hydrogen is a carrier of energy much like water in a heating system and has the potential, with other sources, to help curb the use of fossil fuels. It has a low molecular weight (it is about 8 times lighter that methane representing natural gas) and has a higher energy content per unit mass. At any given pressure, hydrogen gas contains less energy per unit volume than other substances such as methane, methanol, ethanol, propane, and octane. These other substances require various transformation methods before they can be used.

Hydrogen fuels are growing due to the fact that they can be produced from renewable energies such as solar energy, wind, geothermal energy, and hydroelectric power. Using renewable energy makes the process of producing hydrogen carbon free and appealing to environmentally conscience societies. A current problem with using hydrogen fuels is the production of the fuel in an economical fashion.

In contrast with the above-mentioned ill effects on the environment from fossil fuels, hydrogen is the cleanest burning fuel yet. Some of the properties [12], which make hydrogen extremely favorable, are:

- Hydrogen is the most abundant element in the universe, accounting for 90% of the universe by weight.
- It is the lightest element, having a density of 0.08988 grams per liter at standard pressure. (This property is also a disadvantage.)
- It has a high energy content per weight (nearly three times as much as gasoline), but the energy density per volume in gaseous state is quite low at standard temperature and pressure.
- The minimum required ignition energy required for a stoichiometric fuel/oxygen mixture is 0.02 mJ for hydrogen, 0.29 mJ for methane and 0.26 mJ for propane [12].
- Hydrogen has a wide flammability range, burning in air at concentrations in the range of 4 - 75% by volume (methane burns at 5.3 - 15% and propane at 2.1 - 9.5% concentrations by volume) [12].
- The combustion of hydrogen does not produce carbon dioxide ($CO_2$), particulate, or sulfur emissions. However it can produce nitrous oxide (NOX) emissions under some conditions.
- The Higher Heating Value is 134,200 BTU and the Lower Heating Value is 113,400 BTU for 1kg or 2.2 lbs of Hydrogen (which can produce 141 KJ) [12].
- It can be generated from non-fossil sources such as electrolysis of water.

- Post-combustion products do not contain any carcinogenic compounds.

All these features of Hydrogen make it uniquely suitable to replace fossil fuels and are the driving forces to select it as fuel.

## 2.3 Hydrogen Production Technologies

Hydrogen production technologies vary in procedure and complexity. The following sections give an explanations of a few of the various methods used in the formation of hydrogen gas.

### 2.3.1 Electrolysis

Electrolysis the process of making a non-spontaneous process occurs by applying an external power supply to the application [3]. It is also defined as a method of separating chemically bonded elements and compounds by passing an electric current through them. In the case of creating hydrogen, water is separated into oxygen and hydrogen. The amount of energy required depends on the strength of the chemical bond. The energy efficiency of water electrolysis varies widely. The efficiency is a measure of what fraction of electrical energy used is actually contained within the hydrogen. Some of the electrical energy is converted to heat, a useless by-product. Some reports quote efficiencies between 50% and 70% [13]. This efficiency is based on the Lower Heating Value of Hydrogen. The Lower Heating Value of Hydrogen is thermal energy released

when Hydrogen is combusted. This does not represent the total amount of energy within the hydrogen; hence the efficiency is lower than a more strict definition.[2]

Other reports quote the theoretical maximum efficiency of electrolysis. The theoretical maximum efficiency is between 80% and 94% [14]. The theoretical maximum considers the total amount of energy absorbed by both the hydrogen and oxygen. These values refer only to the efficiency of converting electrical energy into hydrogen's chemical energy. The energy lost in generating the electricity is not included. About 4% of hydrogen gas produced worldwide is created by electrolysis, and normally used onsite.

### 2.3.2 Steam-Methane Reformation

Steam reforming of natural gas, sometimes referred to as steam methane reforming (SMR), is the most common method of producing commercial bulk hydrogen as well as the hydrogen used in the industrial synthesis of ammonia. It is also the least expensive method for producing hydrogen [15]. SMR is a three step process to produce hydrogen. Methane is first catalytically reformed at elevated temperature and pressure to produce a syngas mixture of $H_2$ and CO [16]. At high temperatures (700 – 1100 °C) and in the presence of a metal-based catalyst (nickel), steam reacts with methane to yield carbon monoxide and hydrogen as shown in the following equation: $CH_4 + H_2O \rightarrow CO + 3H_2$.

---

[2] The heating value of the fuel, which is defined as the amount of heat released when a fuel is burned completely in a steady-flow process and the products are returned to the state of the reactants. In other words, the heating value of a fuel is equal to the absolute value of the enthalpy of combustion of the fuel. That is,

$$\text{Heating value} = |h_c| \qquad \text{(kJ/kg fuel)}$$

The heating value depends on the phase of the $H_2O$ in the products. The heating value is called the higher heating value (HHV) when the $H_2O$ in the products is in the liquid form, and it is called the lower heating value (LHV) when the $H_2O$ in the products is in the vapor form. The two heating values are related by

$$HHV = LHV + (mh_{fg})_{H_2O} \qquad \text{(kJ/kg fuel)}$$

where m is the mass of $H_2O$ in the products per unit mass of fuel and $h_{fg}$ is the enthalpy of vaporization of water at the specified temperature. [17]

Additional hydrogen can be recovered by a catalytic shift reaction. This is a lower-temperature gas-shift reaction with carbon monoxide produced. The combinations of CO and $H_2O$ produce the $H_2$ product [18]. The reaction is summarized by: $CO + H_2O \rightarrow CO_2 + H_2$

The hydrogen product is then purified by adsorption. The United States produces nine million tons of hydrogen per year, mostly by steam reforming of natural gas [19].

### 2.3.3 Biomass Gasification

Biomass may used to produce hydrogen in two ways: by a direct gasification process, or by pyrolysis to produce liquid bio-oil for reforming. Biomass refers to crops or other agricultural products, including hardwood, softwood, and other plant species. It may also include municipal solid waste or sewage, a fraction of which is burned to produce steam for the process.

When biomass is heated without oxygen or only about one-third the oxygen needed for efficient combustion, it gasifies to a mixture of carbon monoxide and hydrogen—synthesis gas or syngas. The amount of oxygen and other conditions determine if biomass gasifies or pyrolyzes.

The direct biomass gasification process is similar to the coal gasification process. The process is carried out in three steps. First, the biomass is treated with high temperature steam in an oxygen-blown or air-blown gasifier to produce an impure syngas mixture composed of hydrocarbon gases, hydrogen, carbon monoxide, carbon dioxide, tar, and water vapor. Char (carbon residue) and ash are left behind in the gasifier. Then, a portion of the char is gasified by reaction with oxygen, steam, and hydrogen, while another portion is combusted to provide heat. As in the coal gasification process, the

gasification step is followed by the shift reaction and purification [20]. The equations for the three step biomass gasification process are [21]:

Biomass + Energy ↔ Bio-oil + Char + Gas Impurities (pyrolysis)
Bio-oil + $H_2O$ ↔ CO + $H_2$ (reforming)
CO + $H_2O$ ↔ $CO_2$ + $H_2$ (shift reaction)

### 2.3.4 Photoelectrolysis

This is an area of research that is continuing to grow and the shows some promising results. Photoelectrolysis is the conversion of light into a current, and then the division of a molecule using that current. Photoelectrolysis occurs in a photoelectrochemical cell when light is used for electrolysis. This method integrates solar energy collection technologies and water electrolysis into a single photoelectrode. This eliminates the need for a separate power generator and electrolyzer, reducing overall costs and increasing efficiency.

Photoelectrolysis uses photoelectrochemical (PEC) light collecting systems to power the electrolysis of water. When exposed to sunlight, a semiconductor photoelectrode, submerged in an aqueous electrolyte, will generate sufficient electrical energy to promote hydrogen and oxygen evolution reactions (HER and OER).

In order for direct photoelectrochemical decomposition of water to occur, several requirements must be met. The energy band of the semiconductor materials must overlap the energy levels of the hydrogen and oxygen reduction reactions. The semiconductor system must be stable under photoelectrolysis conditions. Finally, the charge transfer from the surface of the semiconductor must be fast enough to prevent corrosion and also reduce energy losses due to overvoltage [22].

### 2.3.5 Hydrogen from Coal—Carbon Sequestering

Like the steam methane reforming process, coal gasification involves three steps. The first step is the treatment of coal feedstock with high temperature steam (1330ºC) to produce syngas, the second a catalytic shift conversion, and third the purification of the hydrogen product.

In the first step, coal is chemically broken down by high temperature (around 1300ºC), high pressure steam to produce raw synthesis gas, as described by the following reaction: coal (carbon source) + $H_2O \leftrightarrow H_2 + CO$ + impurities. In the second step, the syngas passes through a shift reactor converting a portion of the carbon monoxide to carbon dioxide, as shown in the reaction: $CO + H_2O \leftrightarrow CO_2 + H_2$

In the third step, the hydrogen product is purified. Physical absorption removes 99% of $H_2S$ impurities. The majority of $H_2$ in the shifted syngas (85%) is then removed as 99.999% pure $H_2$ in a pressure swing adsorption unit (PSA). In the case of $CO_2$ sequestration, a secondary absorption tower removes $CO_2$ from the remaining shifted syngas. This waste gas is burned to produce electricity.

Partial oxidation of coal is a promising technology for the production of electric power and hydrogen that uses integrated gasification combined-cycle (IGCC) technology. Partial oxidation, or gasification, combines coal, oxygen and steam to produce synthesis gas that is cleaned of impurities such as sulfur or mercury.

To produce hydrogen, this synthesis gas is further processed using mature water-gas shift reactor technology to increase hydrogen and convert carbon monoxide to carbon dioxide. Hydrogen is then separated using PSA technology. Hydrogen production from

coal-derived synthesis gas essentially uses the same gasification process steps currently being developed in DOE's coal-based clean electric power generation program [20].

### 2.3.6 Bio-hydrogen—Bio-hydrogen Methods

Hydrogen can be derived from sunlight, either directly or indirectly from biomass through photosynthesis. This process is represented by the realization of anaerobic and photosynthetic microorganisms using carbohydrate rich and non-toxic raw materials to produce hydrogen. Under anaerobic conditions, hydrogen is produced as a by-product during conversion of organic wastes into organic acids which are then used for methane generation. The acidogenic phase of anaerobic digestion of wastes can be manipulated to improve hydrogen production.

Additionally, volatiles and steam released during the charring of biomass produce hydrogen. This charring turns the biomass into charcoal pieces. This charcoal becomes a nitrogen-enriched fertilizer with the addition of ammonia. This ammonia is formed by combining a third of the hydrogen with nitrogen. The remaining hydrogen can be sold as fuel, both for a hydrogen-based, clean diesel and to run fuel cells.

In order to efficiently produce hydrogen from biomass such as crop wastes, sugar, starch, and oils the development of advanced technologies for biomass reforming is required.

### 2.3.7 Nuclear Methods

Hydrogen production processes that can use nuclear heat or alternative energy sources are endothermic water splitting processes. These processes are generally newer technologies and tend to be more expensive than fossil fuel processes, but do not produce

harmful emissions or consume large quantities of non-renewables. These processes are photocatalytic and photobiological processes that use solar energy, while the sulfur iodine process uses nuclear heat. In the case of electrolysis, electricity supplies the energy required. While this electricity could be produced using fossil fuels, a cleaner alternative is using electricity produced using nuclear heat or an alternative energy processes like wind, solar, or water power [23].

## 2.4 Electrolyzer Technologies

Electrolysis is the process of making a non-spontaneous process to occur by applying an external power supply to the application [3]. In other word hydrogen and oxygen can be achieved by passing an electric current (DC) between two electrodes separated by an aqueous electrolyte with good ionic conductivity. For this reaction to occur a minimum electric voltage must be applied to the two electrodes. Gibbs free energy for water splitting can be used to determine this minimum voltage. The chemical equations for electrolysis are described in Eq. 2.1-2.3. Figure 2.8 shows the process and along with what is needed to produce hydrogen.

The Department of Energy explains that high-temperature electrolysis (HTE), or steam electrolysis as it is sometimes called, is a variation of the conventional electrolysis process. In (HTE) the energy needed to split the water is added in as heat instead of electricity, thus reducing the overall energy required to produce hydrogen and improving process efficiency [24].

$$H_2O(l) + Electrical Energy \Rightarrow H_2(g) + \frac{1}{2}O_2(g) \qquad (2.1)$$

$$\text{Anode: } 2OH^-(aq) \Rightarrow \frac{1}{2}O_{2(g)} + H_2O(l) + 2e^- \tag{2.2}$$

$$\text{Cathode: } 2H_2O(l) + 2e^- \Rightarrow H_2(g) + 2OH^-(aq) \tag{2.3}$$

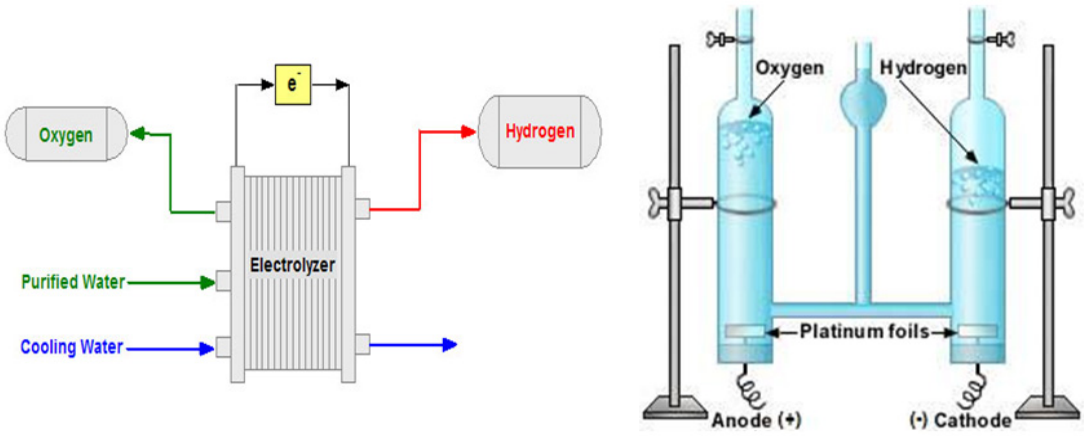


Fig. 2.8: Production of hydrogen from an electrolyzer.

## 2.5 Effect of Feed Water Temperature on Electrolzer Performance

Deab and Mahmound [25] showed experimentally that energy savings per kilogram of $H_2$ gas increases with an increase in the operating fuel cell current. The increase of polarization increases the resistance of the cell. Polarization is the deposit of gases, produced during electrolysis, on the electrodes of a cell. Deab and Mahmound also state that an increase of temperature will lead to a decrease in the polarization needed to sustain the electrolytic process. By Ohm's law when the resistance is decreased the voltage required to sustain the process is decreased thereby increasing the efficiencies.

In the February 2005 issue of Advanced Materials and Processes an article claims that high temperature electrolysis enhances the efficiency of the processes by adding substantial amounts of external heat to the process and by doing so increases the efficiencies by 15-20% [26].

Grigor'ev and Porembskii have discovered that elevated temperatures help reduce power consumption by reducing the resistance of the membrane and the resistance of the process voltage [27].

## 2.6 Geothermal Energy for Producing Hydrogen

Geothermal Energy is a clean domestic energy source that is available 24 hours a day. The average geothermal power plant produces electricity 90% of the time, compared with 65-75% for coal and nuclear-powered plants. Although by itself, geothermal energy will not replace fossil fuels as the major energy source in the United States, it can contribute in a significant way to the nation's energy mix [28]. An objective of this study is to better understand the potential of geothermal resources of the western United States for producing electricity. This electricity will be used for the production of hydrogen. The $H_2$Fuel team assessed that geothermal energy was the most economic for the overall system given the current state of the various renewable energy technologies and RTC requirements for redundancy and reliability. Virtually everything else that $H_2$Fuel will include in the project, i.e., electrolysis fuel production, storage, transmission, distribution, fleet operations, public education, codes and standards, etc., will have direct applications to other production systems that are powered by wind, solar, nuclear, or fossil fuel [29].

Geothermal energy technologies use the heat of the earth for electrical power production, direct use applications, and geothermal heat pumps. The majority of the

available geothermal energy within the United States is concentrated in the western states. Most of these geothermal resources are on public land, which accounts for about 75% of the electrical power generated by geothermal resources [30].

High temperature geothermal systems greater than 300°F offer the greatest output and lowest cost electrical generation. Based on the 1978 geothermal assessment by the U.S. Geological Survey, twelve western states have high temperature geothermal resources. The total high temperature geothermal resource potential in these states is estimated at 22,000 MW. About 2,800 MW of electricity is currently generated using geothermal energy [30].

Geothermal electricity production in the United States began in 1960. Today there are over 20 plants in the western United States providing a total of about 2,200 MW of clean and reliable electricity. Currently identified resources in the U.S. could provide as much as 20,000 MW of power, and undiscovered resources may provide five times that amount [31].

Up to 1,487 MW of new geothermal power plant capacity is currently under development in the United States (including projects in the initial development phase). 223 MW of capacity is currently under construction in 8 projects across the Western United States. Unconfirmed projects (some of which are likely to be developed within the next few years) raise these numbers to 2,051 MW of potential capacity currently under consideration [32]. A quote posted by the geothermal energy association in their guide to geothermal energy states:

> The United States, as the world's largest producer of geothermal electricity, generates an average of 15 billion kilowatt hours of power per year, comparable

to burning close to 25 million barrels of oil or 6 million short tons of coal per year. [33, p.1]

In a paper titled, Geothermal Resource Potential within the State of Nevada it reads:

> It is becoming increasingly clear that it will take multiple energy resources to satisfy the nation's long term energy requirements. Solutions will be a blend of multiple types determined by available local resources, economics, environmental issues, etc. In fact, twenty one states have enacted renewable energy portfolio standards that emphasize local conditions and resources [29, p. 1].

In the geographic area of study, six of the eleven states have ratified renewable energy portfolio standards. Those states are California, Nevada, Arizona, New Mexico, Colorado, and Montana. These six states have taken legislative measures to increase the amount of electricity produced from renewable resources. Table 1 shows the percentage goals of electricity produced by renewable energy by year.


Fig. 2.9: Area of study.

Eligible technologies are Solar Water Heat, Solar Space Heat, Solar Thermal Electric, Solar Thermal Process Heat, Photovoltaic, Landfill Gas, Wind, Biomass, Hydroelectric, Geothermal Electric Power, Municipal Solid Waste, Certain Energy Efficiency Measures, Solar Pool Heating, Anaerobic Digestion, and Biodiesel. However, not less than 5% of the portfolio energy standard must be generated, acquired, or saved from solar energy systems [33].

The Western States share a capacity of almost 13,000 megawatts of geothermal energy that can be developed on specific sites within a reasonable timeframe. Of these, 5,600 megawatts are considered by the geothermal industry to be viable for commercial development within the next 10 years, i.e. by about 2015. This is a commercially achievable capacity for new generation and does not include the much larger potential of unknown, undiscovered resources [34].

Table 2.1: Electric Production Potentials of Geothermal Resources [35]

| Geothermal Electric Production Potential | | |
|---|---|---|
| Alaska | 250 | MW |
| Arizona | 1,000 | MW |
| California | 12,000 | MW |
| Hawaii | 250 | MW |
| Idaho | 540 | MW |
| Montana* | 400 | MW |
| Nevada | 2,000 | MW |
| New Mexico | 2,700 | MW |
| Oregon | 2,200 | MW |
| Utah | 1,350 | MW |
| Washington* | 300 | MW |
| **TOTAL** | **22,990** | **MW** |

*Montana per Dr. John Lund and Washington State estimated by Prof. Gordon Bloomquist.

# Chapter 3

# ELECTROLYZER WATER

## 3.1 Introduction

A critical component of the $H_2$Fuel project is water. Table 1 shows the water requirements for the project as a function of time. Due to the significant nature of these requirements this chapter has been devoted to discussing possible alternatives. The water can be obtained from the city, purchased, or gathered from underground wells. This chapter looks into theses water needs and the conditioning that needs to take place so that the water can be used for the electrolysis process.

Purified water is needed to produce hydrogen and oxygen by electrolysis. The $H_2$Fuel project desires to use water in the projected facility area for this process. Water samples were taken and analyzed from Steamboat Creek at Highway 341 and numerous geothermal wells which included PW-1, PW2, PW-3, IW-2/3, PW2-1, PW2-2, PW2-3, PW2-5, PW3-1, PW3-2, PW3-3, PW3-4, HA-4, IW-4, and SB I Inlet. The data was compiled quarterly from June 2003 to June 2004 and provides helpful information in determining the water needs for hydrogen production within the $H_2$Fuel project.

## 3.2 Background

The Electrolyzers in production call for water that meets the ASTM Type I or II standards. These standards are set forth by An American National Standard. The designation of this standard is Designation: D 1193 – 06 [36] and has been approved for use by agencies of the Department of Defense. These standards are found in Table 3.1.

Table 3.1: ASTM Water Standards

**TABLE 1 Processes for Reagent Water Production**

| Type | Grade | Production Process[A,B,C,D] | µS/cm[E] (max) | MΩ·cm[F] (min) | pH[G] | TOC µg/L[H] (max) | Sodium µg/L[I] (max) | Chloride µg/L[J] (max) | Total Silica µg/L (max) | HBC[K] cfu/mL (max) | Endotoxin, EU/mL[L] (max) |
|---|---|---|---|---|---|---|---|---|---|---|---|
| I | | Purify to 20 µS/cm by dist. or equiv., followed by mixed bed DI, 0.2 µm filtration[A] | 0.0555 | 18 | | 50 | 1 | 1 | 3 | | |
| I | A | Purify to 20 µS/cm by dist. or equiv., followed by mixed bed DI, 0.2 µm filtration[A] | 0.0555 | 18 | | 50 | 1 | 1 | 3 | 10/1000 | 0.03 |
| I | B | Purify to 20 µS/cm by dist. or equiv., followed by mixed bed DI, 0.2 µm filtration[A] | 0.0555 | 18 | | 50 | 1 | 1 | 3 | 10/100 | 0.25 |
| I | C | Purify to 20 µS/cm by dist. or equiv., followed by mixed bed DI, 0.2 µm filtration[A] | 0.0555 | 18 | | 50 | 1 | 1 | 3 | 100/10 | |
| II | | Distillation[B] | 1.0 | 1.0 | | 50 | 5 | 5 | 3 | | |
| II | A | Distillation[B] | 1.0 | 1.0 | | 50 | 5 | 5 | 3 | 10/1000 | 0.03 |
| II | B | Distillation[B] | 1.0 | 1.0 | | 50 | 5 | 5 | 3 | 10/100 | 0.25 |
| II | C | Distillation[B] | 1.0 | 1.0 | | 50 | 5 | 5 | 3 | 100/10 | |
| III | | Distillation, DI, EDI, and/or RO, followed by 0.45 µm filtration.[C] | 0.25 | 4.0 | | 200 | 10 | 10 | 500 | | |
| III | A | Distillation, DI, EDI, and/or RO, followed by 0.45 µm filtration.[C] | 0.25 | 4.0 | | 200 | 10 | 10 | 500 | 10/1000 | 0.03 |
| III | B | Distillation, DI, EDI, and/or RO, followed by 0.45 µm filtration.[C] | 0.25 | 4.0 | | 200 | 10 | 10 | 500 | 10/100 | 0.25 |
| III | C | Distillation, DI, EDI, and/or RO, followed by 0.45 µm filtration.[C] | 0.25 | 4.0 | | 200 | 10 | 10 | 500 | 1000/100 | |
| IV | | Distillation, DI, EDI, and/or RO.[D] | 5.0 | 0.2 | 5.0 to 8.0 | | 50 | 50 | | | |
| IV | A | Distillation, DI, EDI, and/or RO.[D] | 5.0 | 0.2 | 5.0 to 8.0 | | 50 | 50 | | 10/1000 | 0.03 |
| IV | B | Distillation, DI, EDI, and/or RO.[D] | 5.0 | 0.2 | 5.0 to 8.0 | | 50 | 50 | | 10/100 | 0.25 |
| IV | C | Distillation, DI, EDI, and/or RO.[D] | 5.0 | 0.2 | 5.0 to 8.0 | | 50 | 50 | | 100/10 | |

Type I grade of reagent water shall be prepared by distillation or other equal process, followed by polishing with a mixed bed of ion-exchange materials and a 0.2-µm membrane filter. Feed water to the final polishing step must have a maximum conductivity of 20 µS/cm at 298K (25°C).

Type II grade of reagent water shall be prepared by distillation using a still designed to produce a distillate having a conductivity of less than 1.0 µS/cm at 298 K (25°C). Ion exchange, distillation, or reverse osmosis and organic adsorption may be required prior to distillation, if the purity cannot be attained by single distillation.

Type I and II reagent waters may be produced with alternate technologies as long as the appropriate constituent specifications are met and that water so produced has been shown to be appropriate for the application where the use of such water is specified [36].

Table 3.2: Alternative Display of ASTM Water Standards

| | Type I | Type II | Type III | Type IV | Notes |
|---|---|---|---|---|---|
| Electrical conductivity | 0.056 | 1 | 0.25 | 5.0, max | µS/cm at 298 K (25° C) |
| Electrical resistivity | 18 | 1 | 4 | 0.2, min | megohm-cm at 298 K(25° C) |
| pH at 298 K (25° C) | NA | NA | NA | 5.0 to 8.0 | |
| Total organic carbon,ug/L | 50 | 50 | 200 | no limit (TOC), max | |
| Sodium, max, ug/L | 1 | 5 | 10 | 50 | |
| Chlorides, max, ug/L | 1 | 5 | 10 | 50 | |
| Total silica, max, ug/L | 3 | 3 | 500 | no limit | |

## 3.3 Data

Table 3.3: Average Creek Water Data Relevant to ASTM Standards

| Sample taken from Steamboat Creek@ HWY 341 | | | | | |
|---|---|---|---|---|---|
| | Jun-2003 | Sep-2003 | Dec-2003 | Mar-2004 | Jun-2004 |
| TDS [µg/L] | 1.21E+06 | 8.90E+05 | 8.20E+05 | 3.54E+05 | 9.50E+05 |
| Chloride [µg/L] | 4.70E+05 | 3.40E+05 | 3.00E+05 | 8.40E+04 | 3.70E+05 |
| EC [µg/L] | 1.84E+03 | 1.38E+03 | 1.30E+03 | 6.50E+02 | 1.34E+03 |
| Silica [µg/L] | 3.50E+04 | 7.50E+04 | 7.10E+04 | 4.70E+04 | 6.80E+04 |
| Sodium [µg/L] | 3.10E+04 | 2.60E+05 | 2.20E+05 | 7.10E+04 | 2.50E+05 |

Table 3.4: Average Well Water Data Relevant to ASTM Standards

| Sample taken from Geothermal Well Water | | | | | |
|---|---|---|---|---|---|
| | Jun-2003 | Sep-2003 | Dec-2003 | Mar-2004 | Jun-2004 |
| TDS [µg/L] | 2.24E+06 | 2.23E+06 | 2.13E+06 | 2.27E+06 | 2.10E+06 |
| Chloride [µg/L] | 8.30E+05 | 8.30E+05 | 8.53E+05 | 8.50E+05 | 1.40E+06 |
| EC [µg/L] | 3.08E+03 | 3.15E+03 | 3.11E+03 | 3.00E+03 | 3.04E+03 |
| Silica [µg/L] | 2.18E+05 | 2.16E+05 | 2.20E+05 | 2.17E+05 | 2.21E+05 |
| Sodium [µg/L] | 6.27E+05 | 6.23E+05 | 5.87E+05 | 6.10E+05 | 6.71E+05 |

Table 3.5: Average Water Temperature

| | Jun-2003 | Sep-2003 | Dec-2003 | Mar-2004 | Jun-2004 |
|---|---|---|---|---|---|
| Steamboat Creek [°F] | 76 | 64 | 46 | 46 | 61 |
| Geothermal Well Water [°F] | 103.15 | 97.33 | 85 | 85 | 106.79 |

### 3.4 Data Analysis

The geothermal water wells are exceptionally rich in mineral content. While the creek also has a rich mineral content, it contains half that of the wells. Comparing the data with the ASTM water standards shows that the analyzed water will need to be conditioned considerably. The electrical conductivity of the water needs to be reduced by a magnitude of $10^3$ and the other minerals, including sodium, silica, and the chlorides, need to be reduced by a magnitude of $10^6$. The water analysis receive does not provide information on the resistivity or the total organic carbon (TOC), but these values need to be equal to or less than the standards provided by ASTM.

The average temperature of Steamboat Creek during the four quarters was 58.6°F and the average temperature of all the geothermal water wells was 95.45°F. These temperatures are of interest if these water sources are to be used with the electrolyzer. The water needs to be kept at a safe operating temperature to meet with the demands of the production electrolyzer. This temperature range of 40°F to 125°F and is determined by the manufacturer.

### 3.5 Water Consumption

The $H_2$ team has set the goal of 13 kg/day of $H_2$ for the first year of the $H_2$Fuel Project. These hydrogen production goals are outlined by the $H_2$ team [37]. In order to

meet these goals water consumption will need to be on the order of 6 L/hr (1.45 gal/hr) which amounts to 144 L/day (38 gal/day).

### 3.6 Purification Systems

Production electrolyzers require on the order of 100 L/day (26.4 gal/day) to produce an estimated 10 kg/day of $H_2$. There are water conditioning systems available that will meet the requirements and goals of these production electrolyzers and the $H_2$ Fuel Project respectively. Water purification systems such as the Millipore* Super-Q* Plus High-Volume Water Purification Systems, Barnstead* E-pure* 3- and 4-Module Deionization Systems, and Labconco WaterPro Polishing Stations will meet these goals. The first is capable of producing 17280 L/day (4565 gal/day) of purified water. The purifier by Barnstead is capable of 2880 L/day (760 gal/day) and the Labconco system is stated to produce 2590 L/day (684 gal/day) of Type I water. Table 3.6 shows these capabilities and how they compare to the requirements of the electrolyzers. Only a few have been listed to give examples of systems in production. These systems are capable of producing ASTM Type I water in the quantities needed to achieve the $H_2$ Fuel Project goals.

Table 3.6: Water Purification System Capabilities

| Estimated Electrolyzer Water Requirements to produce 10 kg/day of $H_2$ | l/day | gal/day |
|---|---|---|
| | 102 | 26.95 |
| | | |
| Manufacturer | Capabilities | |
| | l/day | gal/day |
| Millipore* Super-Q* Plus High-Volume Water Purification Systems | 17280 | 4565 |
| Barnstead* E-pure* 3- and 4-Module Deionization Systems | 2880 | 760 |
| Labconco WaterPro Polishing Stations | 2590 | 684 |

### 3.7 Recommendations

If this water is to be used for the electrolysis process it will have to be conditioned. Both sources are mineral rich, the wells containing twice as much. It is recommended that two or three stages be used to condition the water. It is recommended that for the first stage a less expensive ion exchange unit should be used to significantly reduce the mineral content. The second recommended stage is a water purification system such as the ones outlined above in order to reach the ASTM standards. A third stage, if necessary, would be a nano-filtration system that polishes the water. After the water goes through these stages it would be suitable for use in the electrolyzer. The primary purpose of the first stage is to increase the life of the membrane cartridges in the water purification system. The mineral rich water will reduce the life expectancy of these membranes quickly if the mineral content of the water if not reduced before arriving at the water purification system. By using a lesser ion exchange unit before the water purification system, the membranes of the expensive unit are preserved for a longer period of time.

### 3.8 Economics

Initially, the costs involved in such a system are the capital costs of the equipment; the ion exchanger, the water purification system, and the polishing equipment are estimated to be on the order of $10,000. Costs afterwards will consist of replacing the filters and membranes of the system and monitoring the quality of the water. Replacement costs of the ion exchange filters will be considerably less than those of the water purification system, another benefit to using an ion exchanger. Another option to consider is that of purchasing the purified water locally and having it shipped to the $H_2$

production facility. Storage as well as plumbing from the storage to the electrolyzer would be necessary. These costs need to be considered and compared to that of purchasing a water purification system in order to make an accurate assessment of how the purified water is going to be obtained.

### 3.9 Conclusions

The analysis of the water data gathered does not meet the water requirements for production electrolyzers. The water from the test sites need to be purified and conditioned considerably in order to be used with the production electrolyzers. This purification can be achieved with modern purification systems to obtain the quality of water required to produce hydrogen efficiently using the methods outlined above. An economic assessment needs to be done to determine whether it is more economical to purchase the water locally or to purify it at the production facility.

# Chapter 4

# GEOTHERMAL HYDROGEN PRODUCTION SYSTEM

## 4.1 System Schematic

Figure 4.1 is a system schematic depicting the basic components of the geothermal hydrogen production system. The main components of the hydrogen production systems are the geothermal plant, electrolyzer, and the heat exchangers. The previous chapter addressed the issue of the water used for the production of hydrogen. As an important part of $H_2$ production the water quality needs to be the best it can, therefore a water filtration unit and a water conditioning unit were included in the model. The water filtration unit will reduce the effects fouling has on the amount of heat exchanged and increase the time intervals for cleaning the heat exchanger, thus reducing maintenance costs. This first filtration component will also increase the life of the water conditioning unit before the electrolyzer.

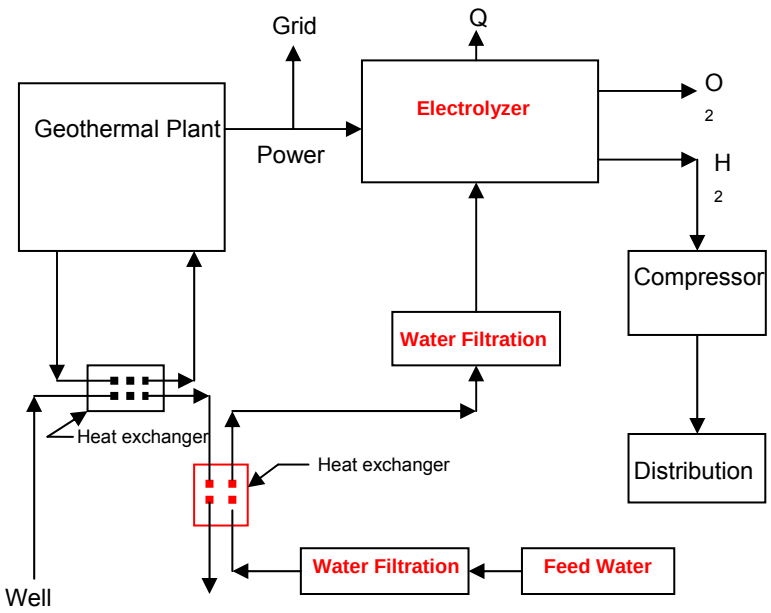


Fig. 4.1: Schematic of the geothermal hydrogen production system.

## 4.2 TRNSYS Model

As previously mentioned, to achieve the objectives of this paper the modeling program named TRNSYS was used. TRNSYS is a simulation environment for the transient simulation of energy systems. The TESS, STEC, and standard TRNSYS libraries were used to create the energy models [6-8]. There are essentially two parts to the model; the geothermal plant and the electrolyzer. The geothermal plant is a simple Rankine cycle which uses the energy from the geothermal wells to create power. The electrolyzer is an alkaline model that produces hydrogen from water.

### 4.2.1 Geothermal Model

As mentioned above the geothermal plant is modeled as a simple rankine cycle operating at steady state. This cycle consist of a boiler section followed by three turbine stages with two extraction lines. A condenser is connected to the final stage of the turbine and a condenser pump follows the condenser. The two extraction splitters are connected to a deaerator and a feedwater heater. A feedwater pump and heat exchanger complete the cycle. The base assumptions made in this model are:

1. Plant operates at steady states
2. Water is an incompressible fluid
3. Gas and liquid are separate phases
4. Kinetic and potential energy changes in the flow loops are negligible.

The TRNSYS simulation studio allows you to place the components of the model as the user see fit. Connections are then made between the components and the parameters and inputs are then established by the user. Figure 4.2 displays the model as it would appear to the user. Initial parameters for the program are listed in Table 4.1. The time step is set at an hour in order to establish a steady state response of the plant model.

Table 4.1: Global Card for TRNSYS Model

| | | |
|---|---|---|
| Simulation start time | 0 | hr |
| Simulation stop time | 168 | hr |
| Simulation time step | 1 | hr |
| Solution method | successive method | - |
| The minimum relaxation factor | 1 | - |
| The maximum relaxation factor | 1 | - |
| Equation solver | 0 | - |
| Equation trace | FALSE | - |
| Debug mode | FALSE | - |
| Tolerance integration | 0.001 | dimensionless |
| Tolerance convergence | 0.001 | dimensionless |
| Tolerance values | Relatives | - |

Flash steam plants are the most common type of geothermal power generation plants in operation. They typically operate with water temperatures greater that 360°F (182°C). The geothermal water is pumped under high pressure to the generation equipment at the surface. In this model the steam input is 200°C with a flow rate of 18 kg/s. The other input is the return temperature from the cooling tower. This temperature is set at 25°C. All other values are computed by TRNSYS. The economizer and superheater are modeled as a zero capacitance cross flow heat exchangers and are sized using the overall heat exchanger coefficient. The pumps are set with flow rates of 50 kg/s. The turbine is a three stage model with two splitters. One splitter diverts flow to a steam condenser while the other diverts flow to a deaerator. The steam condenser then

cools the steam before returning it to the economizer. The same process goes on in the deaerator, but at lower temperatures.

The equations used throughout the system are those explained by the first and second laws of thermodynamics. They use flow rates, temperatures, qualities, enthalpies, and specific heats of steam and water for their calculations of heat and energy transfer. These values are either inputs into the different components or calculated values.

The economizer, superheater, and subcooler are modeled as a zero capacitance counter flow sensible heat exchanger. The cold side input is assumed to be water/steam depending on the quality. The respective specific heat of the cold side fluid is calculated from water/steam property data. The effectiveness is calculated by using the overall heat transfer coefficient (UA). UA is then evaluated from the power law [5-8].

The condenser model is a water cooled condenser. The cooling water temperature rise is set at 10°C. The temperature difference between cooling water outlet temperature and condensing temperature is 5°C. Therefore, the condensing pressure depends only on the feedwater inlet temperature which is constant when the feedwater inlet temperature it is constant.

This turbine stage model calculates the inlet pressure of the turbine stage from the outlet pressure, the steam mass flow rate, and reference values of inlet and outlet pressure and mass flow rate using Stoidolas law of the eclipse. It evaluates the outlet enthalpy from the inlet enthalpy and inlet and outlet pressure using an isentropic efficiency.

The deaerator model describes a mixing water preheater under steady state conditions. It has three inlets and one outlet. The inlet is the feed water flow. A condensate water flow which may come from a preheater at a higher pressure

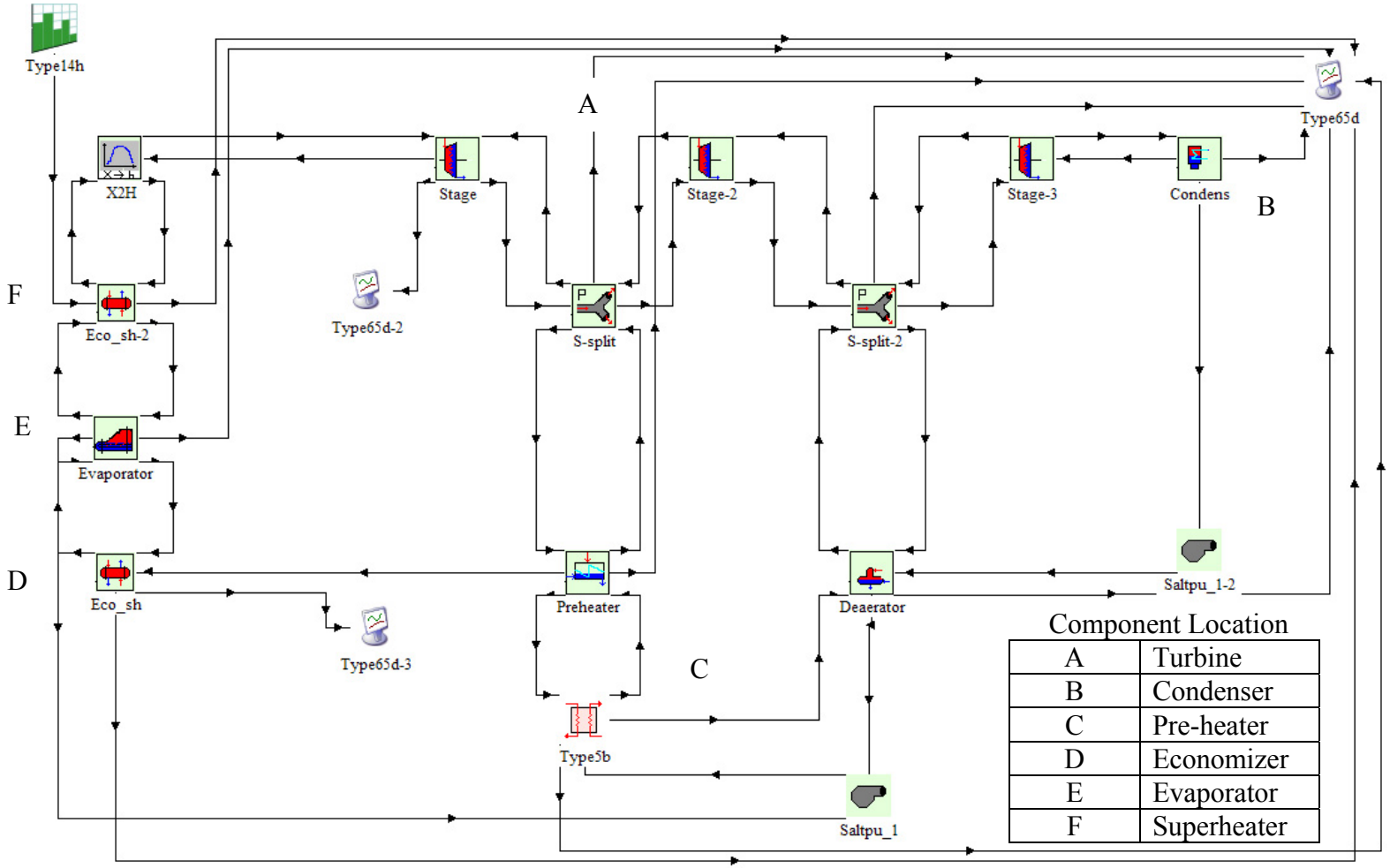


Fig. 4.2: TRNSYS model of the geothermal plan.

level and the steam flow. Outlet is water flow under saturated conditions.

The steam condenser or preheater model assumes water with constant heat capacity on the cold side and condensing steam on the hot side. It calculates the required steam mass flow rate that would keep the water level in this heat exchanger constant. The heat transfer characteristic is described by an effective heat transfer factor (UA). UA is evaluated as a function of the cold side flow rate.

The evaporator simulates a water evaporator, giving outlet temperatures and flow rates of hot and cold streams as well as demanding for a certain water inlet flow rate to obtain total evaporation. The cold side is assumed to be water/steam depending on the quality. Water/Steam conditions are given by temperature, pressure and quality. The effectiveness method is used to describe the heat transfer using an overall heat transfer factor UA. The value for UA is evaluated as a function of the steam flow.

The outputs are then plotted using the online graphics component. This component is used to display selected system variables while the simulation is progressing. This component is highly recommended and widely used since it provides valuable variable information and allows users to immediately see if the system is not performing as desired. These print outs give the user a quick understanding of whether or not the program is running correctly. It also provides output values of the system. A display of this output is shown in Fig. 4.6.

### 4.2.2 Electrolyzer Model

The electrolyzer model in this simulation is for a high pressure alkaline water electrolyzer. It is based on fundamental thermodynamics, heat transfer theories, and empirical electrochemical relationships. The basis of the electrochemical model is a

temperature dependent current-voltage curve for a given pressure, a Faraday efficiency relation independent of temperature and pressure. A dynamic thermal model is also included. The base assumptions made in this model are:

1. Hydrogen and air are ideal gases
2. Water is an incompressible fluid
3. Gas and liquid are separate phases

Using these assumptions the enthalpy, entropy, and Gibbs energy, ΔH, ΔS, and ΔG respectively can be determined for pure hydrogen ($H_2$), oxygen ($O_2$), and water ($H_20$) at standard temperature and pressure (25°C and 1 atm) using standard thermodynamic property tables. The change in Gibbs energy is expressed by Eq. 4.1.

$$\Delta G = \Delta H - T_{ely} \cdot \Delta S \tag{4.1}$$

As explained above, electrolysis is a non-spontaneous reaction. In a non-spontaneous reaction the Gibbs energy is positive. At constant temperature and pressure the maximum possible useful work is equal to the change in Gibbs energy ΔG. The chemical conversion rate in molar quantities is then related to the electrical energy (emf) needed to split water according to Faraday's law. The reversible cell voltage (per cell) for a reversible electrochemical process is:

$$U_{rev} = \frac{\Delta G}{n \cdot F} \tag{4.2}$$

The energy needed to split water is equal to ΔH. This total energy needed is then related to the thermoneutral voltage (per cell) by Eq. 4.3.

$$U_{tn} = \frac{\Delta H}{n \cdot F} \tag{4.3}$$

At standard conditions $U_{rev}$ = 1.229 V and $U_{th}$ = 1.482 V. This change with temperature and in the range of temperatures for electrolyzers $U_{rev}$ increases slightly

while $U_{th}$ remains fairly constant. This can be compensated for by increasing the pressure. This will cause $U_{rev}$ to slightly rise and $U_{tn}$ will remain constant.

Electrolyzers can be modeled using empirical current-voltage (I-U) relationships. Temperatures, overvoltages, and ohmic resistance need to be considered to properly model an electrolyzer. These values are accounted for in the following equations [38]. The Current-Voltage Characteristic (per cell) is:

$$U_{cell} = U_{rev} + r' \cdot \frac{I_{ely}}{A} + s' \cdot \log\left[\frac{t' \cdot I_{ely}}{A} + 1\right] \tag{4.4}$$

with

$$r' = r_1 + r_2 \cdot T_{ely} \tag{4.5}$$

$$s' = s_1 + s_2 \cdot T_{ely} + s_3 \cdot T_{ely}^2 \tag{4.6}$$

$$t' = t_1 + \frac{t_2}{T_{ley}} + \frac{t_3}{T_{ely}^2} \tag{4.7}$$

The Faraday Efficiency is defined as the ratio of the actual vs. the theoretical maximum amount of $H_2$ produced by the electrolyzer. A lower resistance is achieved when the parasitic current[3] increases with decreasing current densities. This happens because of an increasing share of electrolyte. Due to Eq. 4.4, the parasitic current is linear to the cell potential within the cell. This linearity causes the fraction of parasitic currents and total currents to increase with decreasing current densities. Lower

[3] Parasitic currents are unphysical currents generated when using implementations of the continuum surface force (CSF) technique to model surface tension forces in multi-phase computational fluid dynamics problems (CFD). Parasitic currents are unphysical currents generated in fluid regions adjacent to an interface by local variations in the CSF body force. Their magnitude generally increases with increasing capillary strength, and may become so large as to affect the prediction of flow field velocities, or in more dire circumstances, cause complete breakup of an interface [39].

resistance, more parasitic current losses, and lower Faraday efficiencies can be achieved with an increase in temperature. This is demonstrated below.

$$\eta_f = \left[ \frac{I_{density}^2}{a_1 + I_{density}^2} \right] \cdot a_1 \tag{4.8}$$

Faraday's law shows that the rate of $H_2$ production is directly proportional to the transfer rate of the electrons at the electrodes. This also shows that the $H_2$ production rate is proportional to the current in the circuit (Fig. 4.3). An electrolyzer with cells in series will then have a hydrogen production rate calculated by the following equation:

$$\dot{n}_{H_2} = \eta_f \cdot N_{cells} \cdot \frac{I_{ely}}{n \cdot F} \tag{4.9}$$

Electrical inefficiencies are the cause of heat generation in an electrolyzer [40]. The energy efficiency can be calculated with $U_{rev}$ and $U_{th}$ in the following equation:

$$\eta_e = \frac{U_{tn}}{U_{cell}} \tag{4.10}$$

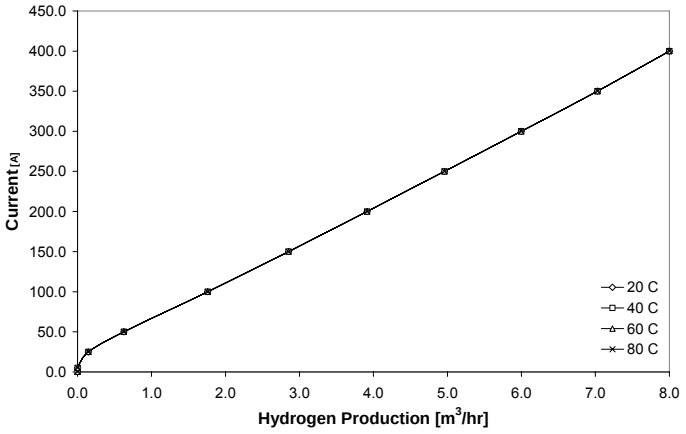


Fig. 4.3: Electrolyzer current [A] vs. $H_2$ production as a function of temperature.

The temperature of the electrolyzer be determined using simple or complex thermal models, depending on the need for accuracy. Assuming a lumped thermal capacitance model, the overall thermal energy balance can be expressed as a linear, first order, non-homogeneous differential equation. The model presented below is calculated on a per stack basis. For this model the overall balance is:

$$C \times \frac{dT}{dt_{ely}} = \dot{Q}_{gen} - \dot{Q}_{loss} - \dot{Q}_{cw} \tag{4.11}$$

The generated thermal energy then becomes:

$$\dot{Q}_{gen} = N_{cells} \times I_{ely} \times [U_{cell} - U_{tn}] \tag{4.12}$$

The heat looses to the surrounding are:

$$\dot{Q}_{loss} = \frac{1}{R_T} \times [T_{ely} - T_{amb}] \tag{4.13}$$

The auxiliary cooling requirements are:

$$\dot{Q}_{cw} = C_{p,H_2O} \times [T_{cs,out} - T_{cw,in}] \tag{4.14}$$

The total electrolyzer efficiency is then determined by:

$$\eta_{tot} = \eta_e \cdot \eta_f \tag{4.15}$$

In this project TRNSYS will use the above equations to model characteristics the hydrogen production unit. An electrolyzer model was created using TRNSYS. The parameters and inputs used in the model are found in Table 4.1. The electrolyzer temperature and currents were varied.

Table 4.2: Electrolyzer Parameters

| Parameters | |
|---|---|
| Electrode area | 0.25 $m^2$ |
| Number of cells | 50 |
| Number of stacks | 1 |
| Current density max. | 300 $mA/m^2$ |
| Temperature max. | 80°C |
| Cell voltage min. | 1.229 V |
| Thermal resistance | 0.167 Ω |
| Thermal time constant | 29 hr |
| Inputs | |
| Electrolyzer pressure | 7 bar |
| Room temperature | 20°C |
| Temp. of cooling water | 15°C |
| Flow rate of cooling water | 0.25 $m^3/hr$ |

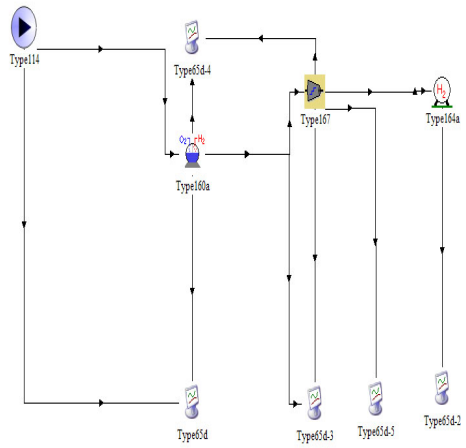


Fig. 4.4: TRNSYS electrolyzer simulation model of Fig. 4.1

### 4.2.3 Combined Geothermal and Electrolyzer Models

The combined model merges the geothermal model with that of the electrolyzer. This is pictured below in Fig. 4.5. The waste water from the plant that leaves the electrolyzer is connected to a heat exchanger which in theory will reduce the temperature of the water using the preconditioned water for the electrolyzer. This will allow energy to be transmitted to the water that the electrolyzer uses to produces hydrogen. As explained above the amount of electrical energy required will then be reduced and thus the efficiencies of producing the hydrogen will increase. The results from these models as well as a discussion of the results can be found in the following chapters. The TRNSYS models described above correspond well to previous studies that employ other programs and methods of analysis.

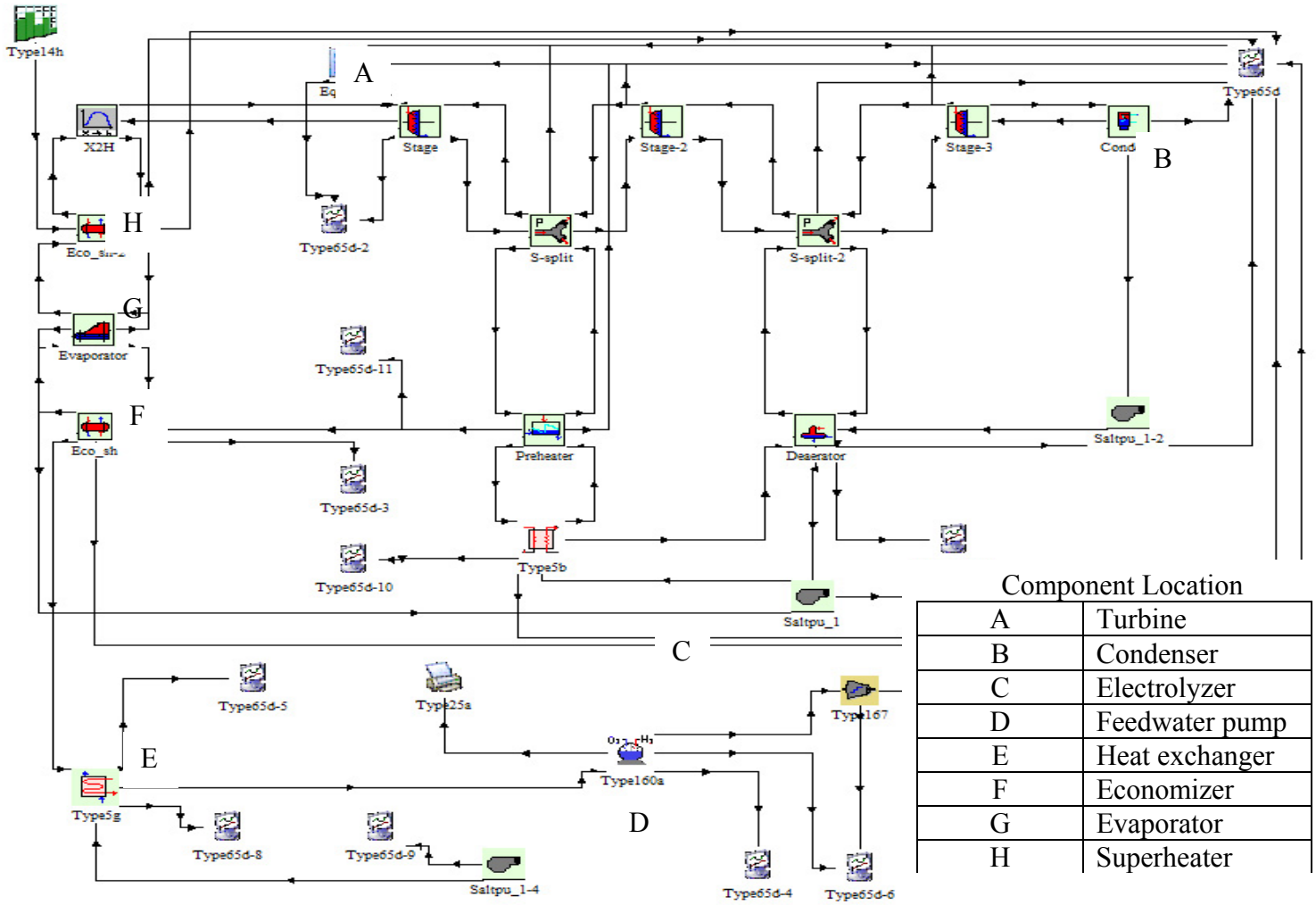


Component Location

| | |
|---|---|
| A | Turbine |
| B | Condenser |
| C | Electrolyzer |
| D | Feedwater pump |
| E | Heat exchanger |
| F | Economizer |
| G | Evaporator |
| H | Superheater |

Fig. 4.5: Depiction of the combined geothermal and electrolyzer models.

## 4.3 Model Validation

One of the objectives of the proposed research is to model an electrochemical process and determine gains and or losses in efficiency of the process by increasing or decreasing the temperature of the feed water. In order to do this geothermal energy was selected as the source of power and energy [4]. For the purposes of the research, the geothermal plant was modeled as a fixed parameter. Research was done to accurately estimate the well temperature of a geothermal well in the area proposed for the $H_2$Fuel project. Once this was established, the plant was assumed to operate at steady state and thus became a fixed parameter. As a fixed parameter other variable could then be adjusted with efforts to accurately determine gains and or losses in the efficiency of the electrochemical process.

By modifying the input parameters of the above geothermal model one can verify the steady state performance of the components. The TRNSYS model is verified by the commercial Computer Code KPRO program [41]. This program was used to evaluate the thermodynamic design performance data of a fictive Rankin cycle. These results are presented in Table 4.2 and shown in Fig. 4.6. The results of the TRNSYS code and its deviation from KPRO are presented for temperature, pressure, and mass flow rate at all relevant locations of the plant. The calculation was based on equal overall heat transfer factors for all heat exchanger units, equal reference pressure losses, and the same inner turbine efficiencies, turbine reference mass flow rates and reference pressures. Figure 4.7 and Table 4.3 show that the conformity of both codes is excellent. For the electrical power output, there was a 0.6% difference between the values computed by each code. Slight differences may result from different formulations of the property functions [8].

Table 4.3: Results from TRNSYS and KPRO

| Component | Temperature [°C] | |
|---|---|---|
| | TRNSYS | TRNSYS code[4] and its deviation from KPRO |
| Dearator | 146.1 | 151.8 + 0 |
| Subcooler | 154.3 | 157.4 + 1.7 |
| Preheater | 203.4 | 207.8 - .4 |
| Economizer | 306.1 | 306.6 + .1 |
| Evaportator | 311.4 | 311.7 + 0 |
| Superheater | 500.1 | 499.9 + .1 |

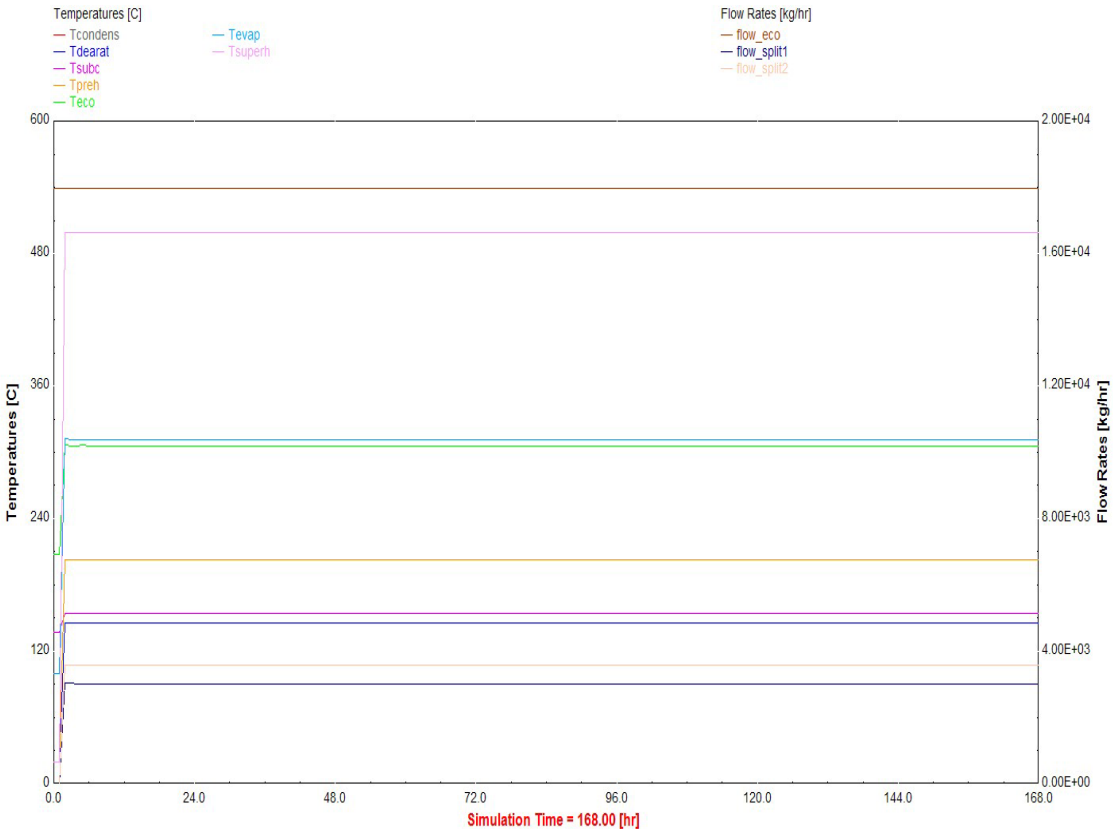


Fig. 4.6: Example of TRNSYS simulation outputs of geothermal plant.

[4] TRNSYS code from the library for Solar Thermal Electric Components (STEC)

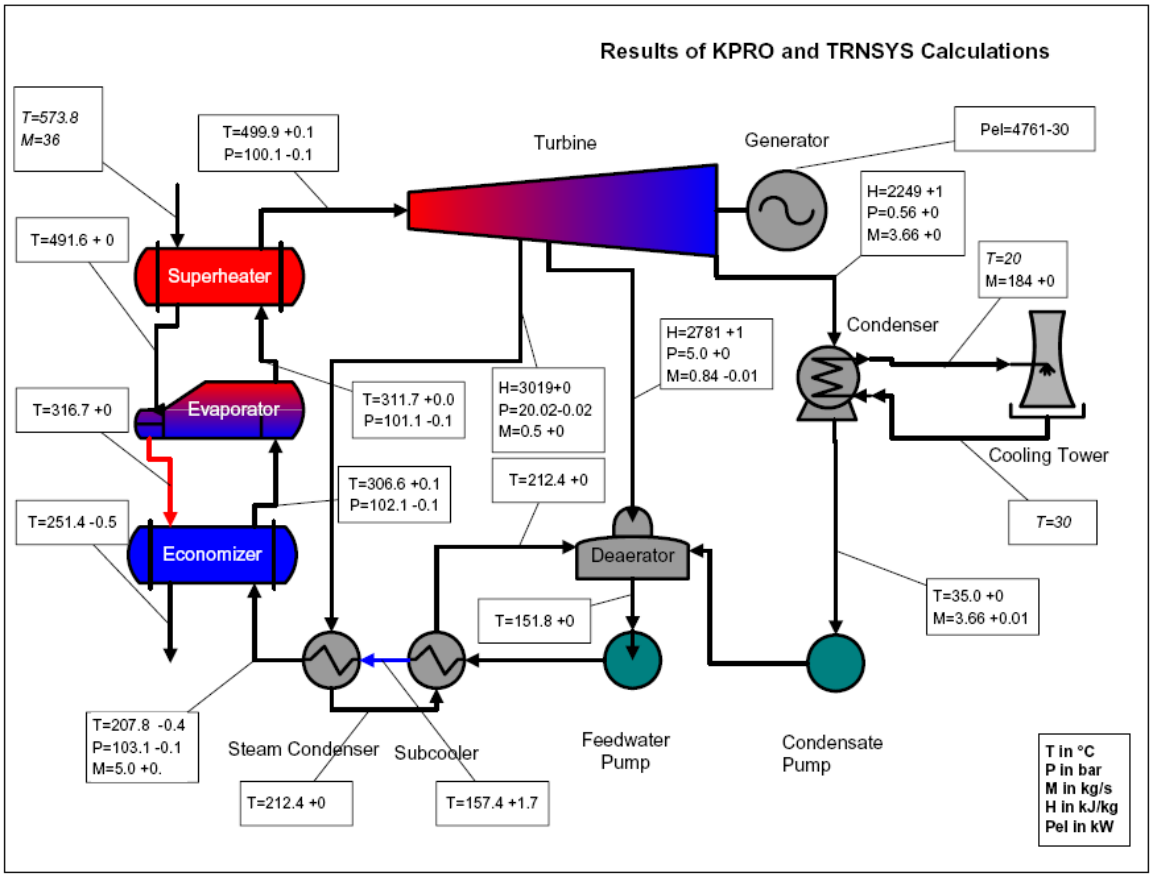


Fig. 4.7: Results from TRNSYS for the geothermal plant model.

A TRNSYS solar hot water heater model can be found in the appendix. The objective of the model was to develop a simple solar water heating model. This model was compared against *F-Chart* results [42] as well as industry standards set forth by the Solar Rating & Certification Corporation [43] to determine the accuracy of the program and the modeling techniques employed by the programmer.

Based on the validations from KPRO and the solar hot water heater model, it can be concluded that the model created for the purposes of the prescribed research can be used with confidence and that the subsequent analysis will reflect real life scenarios.

# Chapter 5

## THE EFFECT OF TEMPERATURE ON THE EFFICIENCIES OF THE ELECTROLYSIS

High temperature electrolyzers (HTE) operate at temperatures between 750°-950°C and low temperature electrolyzers operate at temperatures between 50°-80°C. It can be shown using first and second laws of thermodynamics that energy can be added through heat to improve the electrolyzer efficiency. It is proposed that this energy comes from the waste water of the geothermal plants before it is injected back into the well (Fig. 4.1). Typical binary geothermal plants operating on a Rankine Cycle have injection well temperatures of approximately 80°C and flow rates of approximately 150 kg/s. Commercially available electrolyzers require on the order of 100 L/day (26.4 gal/day) of water to produce 10 kg/day of $H_2$. At these temperatures and flow rates, the water entering the electrolyzers can range from 20°C to 80°C. As shown in Fig. 5.1, when producing 10 kg/day of $H_2$, an increase of 10°C in temperature produces a 0.048 kW increase of energy to the process. This energy could then be used as a supplement to the electricity provided.

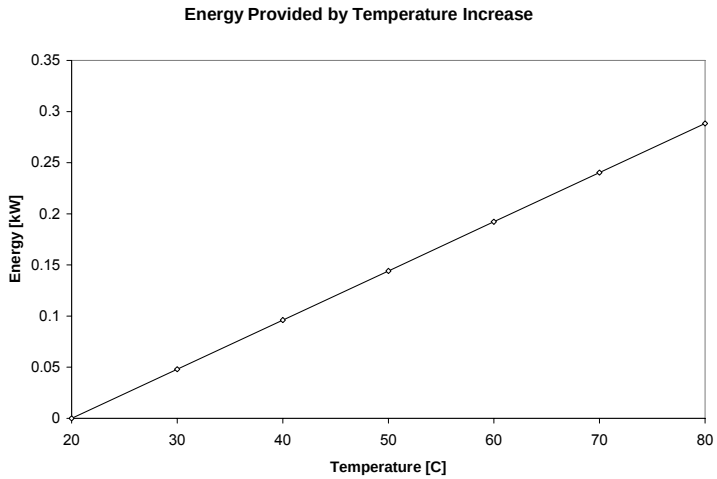


Fig. 5.1: Energy gains are a function of temperature.

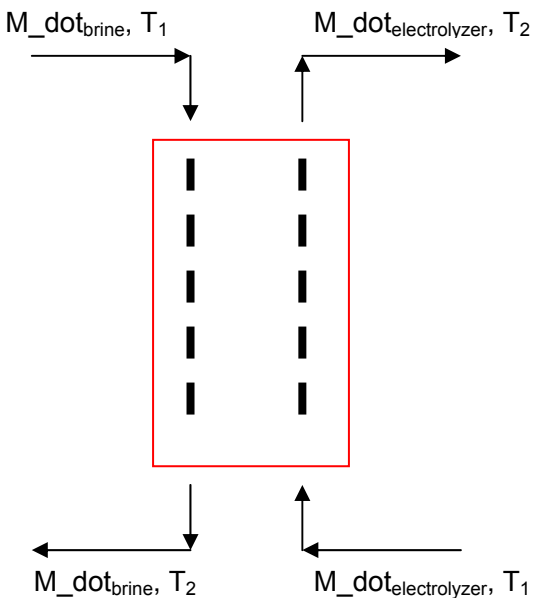


Fig. 5.2: Energy exchange between geothermal brine and electrolyzer feed stock.

## 5.1 Geothermal Model Results

As stated in the previous chapter, the model for the geothermal plant was set with an inlet temperature of 200°C and a flow rate of 18 kg/s. The inputs were determined based on private conversations with Ormat [44]. Ormat is a company dedicated to providing solutions for geothermal power. Ormat has and operates a power plant in Steamboat, Nevada with two other plants planned. These are in the regions considered in the $H_2$Fuel project. The superheater was set with an overall heat exchangers coefficient of 27.2 kW/K. The economizer is modeled as a heat exchanger that has an overall heat exchanger coefficient of 108.3 kW/K. An overall heat exchanger coefficient of 5.9 kW/K was set for the subcooler [5-8]. The cooling tower has an input of 25°C. The overall results of the simulation are summarized in Table 5.1. The power generated by the plants is estimated by TRNSYS as 2.4 MW.

Table 5.1: TRNSYS Steady State Outputs of Combined Model

| TRNSYS STEADY STATE OUTPUTS | | | | | | |
|---|---|---|---|---|---|---|
| Component | Temperature Hot [°C] | Temperature Cold [°C] | Inlet Pressure [Bar] | Flow Rate Hot [kg/hr] | Flow Rate Cold [kg/hr] | Heat Transfer Rate [kJ/hr] |
| Superheater (Counter-Flow Exchanger) | 198.6 | 200 | | 64800 | 1107 | 96340 |
| Economizer (Counter-Flow Exchanger) | **161.4** | 165.6 | | 64800 | 1107 | 283755 |
| Evaporator | 165.5 | 165.5 | 8.162 | 64800 | 1107 | |
| Preheater | 105.8 | 105.8 | | 90.55 | 1107 | |
| Subcooler (Counter-Flow Exchanger) | 71.84 | 74.64 | | 90.55 | 1107 | 12879 |
| Dearator | | 71.85 | | 2109 | | |

| Component | Temperature Hot [°C] | Temperature Cold [°C] | Flow Rate Hot [kg/hr] | Flow Rate Cold [kg/hr] | Heat Transfer Rate [kJ/hr] | Effectiveness |
|---|---|---|---|---|---|---|
| Electrolyzer Heat Exchanger | 28.99 | 78.27 | 64800 | 168000 | 40974000 | 0.9364 |
| Feed Water Pump | | 20 | | | | |
| Electrolyzer | **78.27** | | | | | |

| Component | Inlet Pressure [Bar] | Flow Rate Hot [kg/hr] | Power [MW] | Efficiency |
|---|---|---|---|---|
| Turbine | 6.163 | | 2.38 | 0.8 |
| Splitter 1 | 1.263 | 89.56 | | |
| Splitter 2 | 0.3404 | 141.4 | | |

## 5.2 Analysis

As stated in Chapter 4, the electrolyzer used in the model is a high pressure alkaline water electrolyzer. The following data was gathered by running the simulation described in chapter 4 for various temperatures and current inputs. The temperature was varied from 20-80°C. These were the limits of the TRNSYS electrolyzer component model. They are based on research done by users on actual electrolyzers in production. The current was varied from 50-350 amps during model simulations. This data is depicted in the following charts.

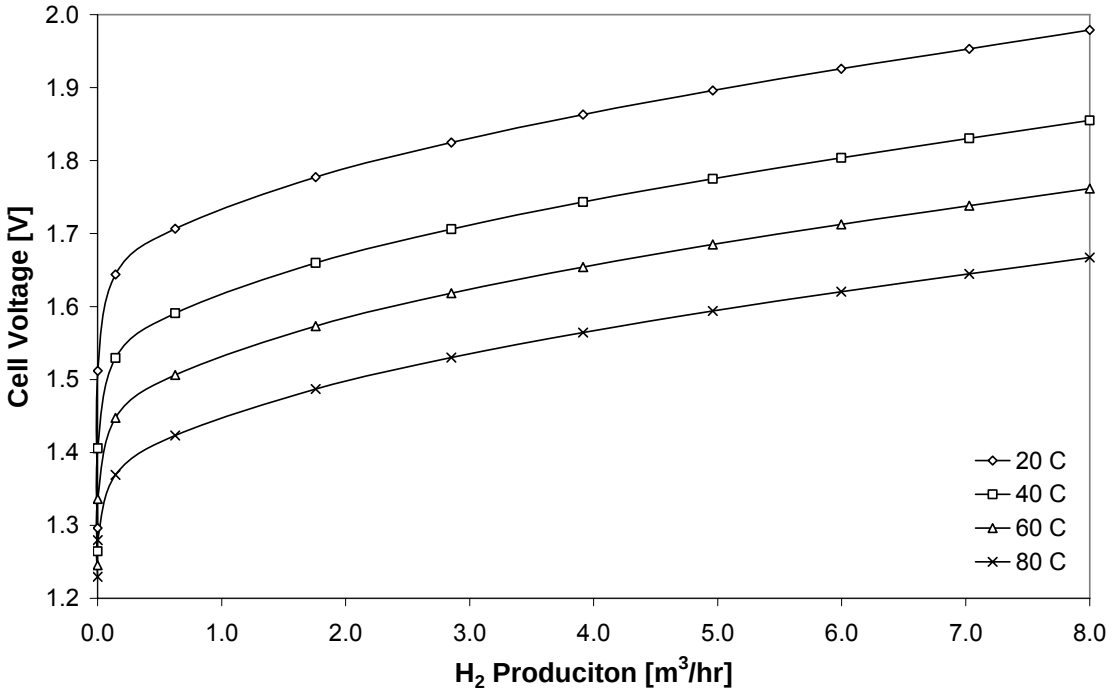


Fig. 5.3: Cell voltage vs. $H_2$ production as a function of temperature.

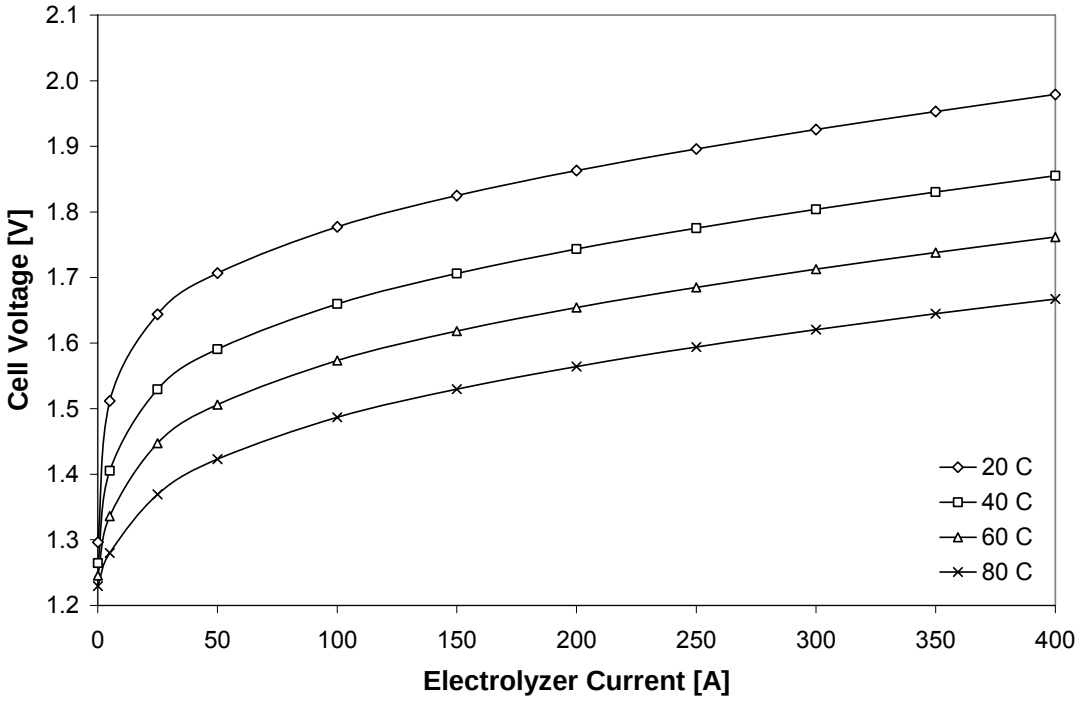


Fig. 5.4: Cell voltage vs. current as a function of temperature.

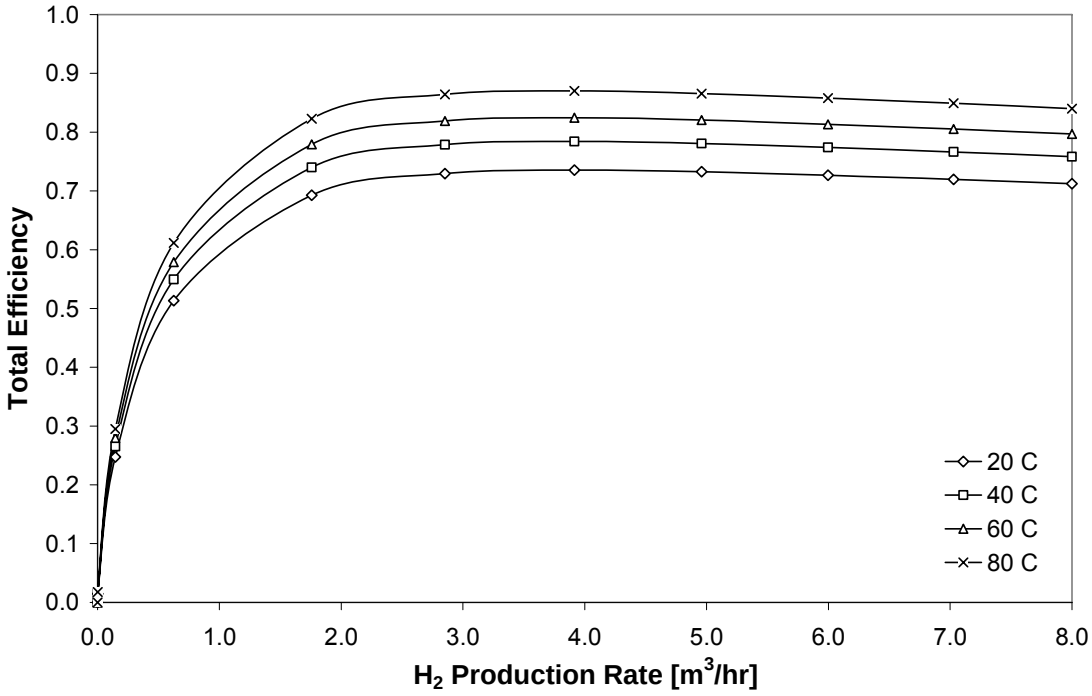


Fig. 5.5: $H_2$ production vs. total efficiency as a function of temperature.

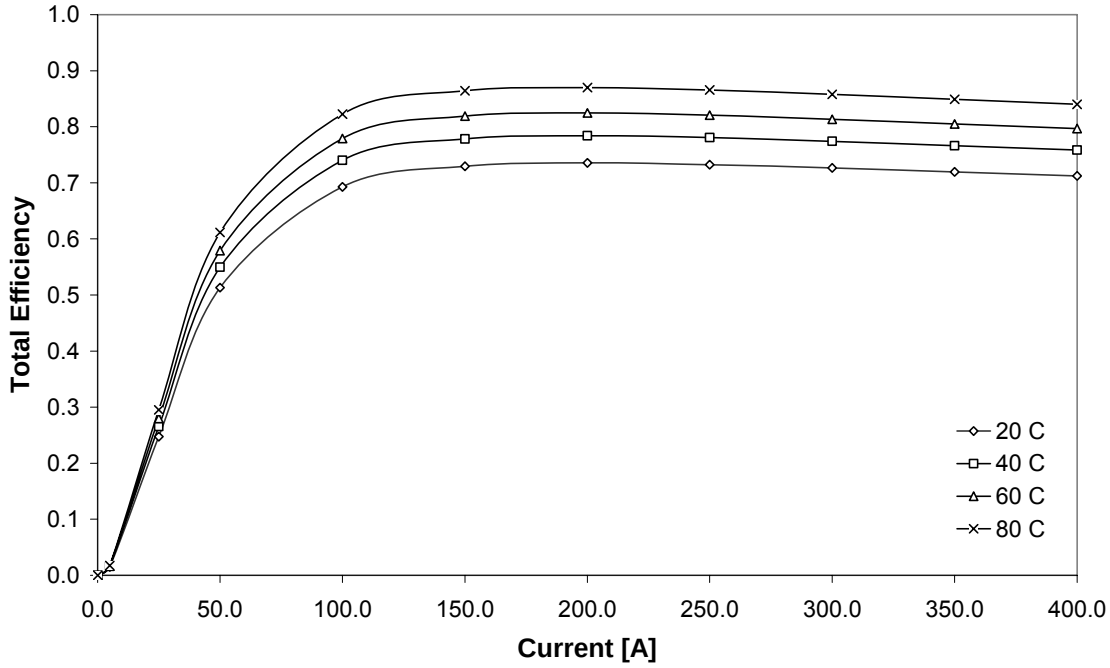


Fig. 5.6: Total efficiency vs. current as a function of temperature.

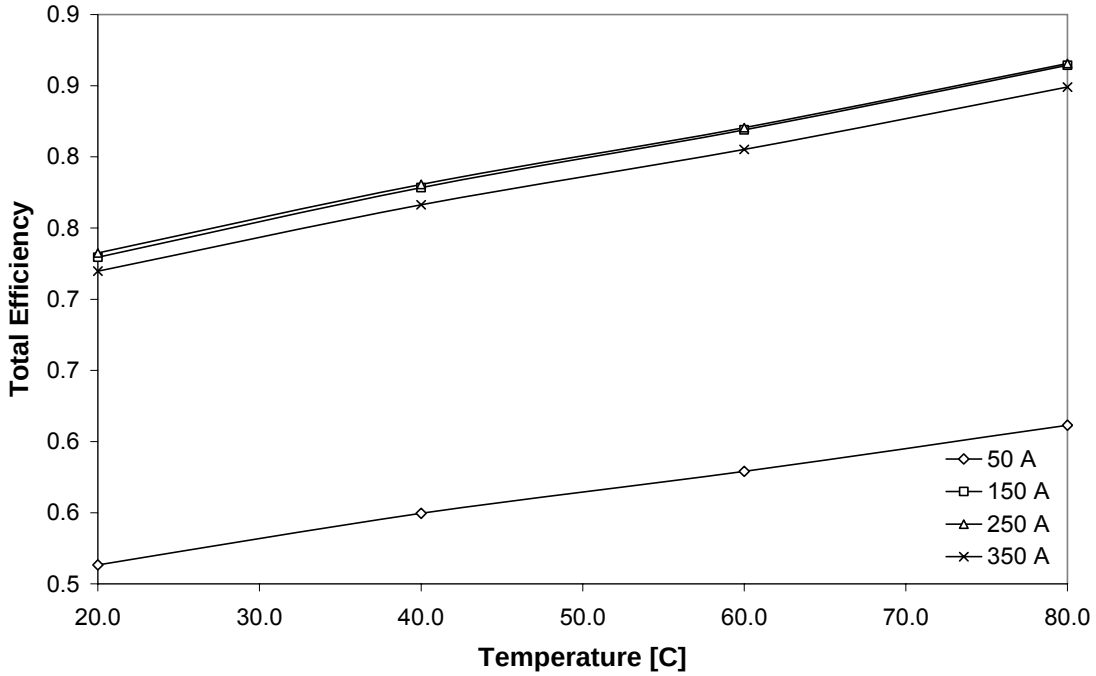


Fig. 5.7: Total efficiency vs. temperature as a function of current.

Figure 4.3 reflects Faraday's law in that hydrogen production is directly proportional to the current density as written above. As shown in Fig. 5.3, for a given current through the electrolyzer stack, the cell voltage decreases as the temperature increases.

It can also be seen that for a given temperature, increasing the hydrogen production, (which is directly proportional to the current density see equation 12) will increase the cell voltage. This is also evident in Fig. 5.4. This increase in the cell potential will cause a decrease in the energy efficiency.

Although the energy efficiency decreases with the increase of the hydrogen production rate, the total efficiency increases as shown in Fig. 5.5. This is because the Faraday efficiency increases with the increase of the current density. This increase is greater than the decrease of the energy efficiency and due to Eq. 4.15, the overall efficiency increases. Figure 5.5 also shows that there is a peak in efficiency. This peak comes at a $H_2$ production rate of more than $4m^3/hr$. An increase in $H_2$ production beyond $4m^3/hr$ will cause the overall efficiency to decrease.

Figure 5.7 shows the temperature vs. total efficiency as a function of current. It is important to not that these total efficiencies take into account a thermodynamic and electrochemical model of an electrolyzer. This includes the cooling water which is of little significance to the overall efficiencies. Less than 2% of electrolyzer power is transferred to the cooling water. This figure also shows an optimum value for the current. When the current becomes too large; the overall efficiency will decrease as shown in Figures 5.5 and 5.7.

Modeling the energy system with TRNSYS allowed for the successful simulation of a hydrogen production facility. By fixing the geothermal plant, analysis of the electrolyzers were performed. The results of the analysis enabled the objectives of the research to be accomplished.

# Chapter 6

# CONCLUSIONS AND RECOMMENDATIONS

## 6.1 Summary

There are many factors involved in the scope of the research being discussed: geothermal potentials, water conditions, electrolyzers, and the complexity of assembling these components in an effort to achieve the objective of this research. In using the TRNSYS program for modeling, the entire energy system including the electrolyzer, geothermal plant, feed water pumps, and storage considerations were modeled and accurate assumptions of a real life system were included. TRNSYS is made up of components created by users in the industry and many of them have been validated using experienced data. Thus, TRNSYS can be used with confidence.

Chapter 3 describes the critical nature of water in the $H_2$Fuel project. Table 1.1 shows the water requirements for the project as a function of time. Due to the significant nature of these requirements Chapter 3 was devoted to discussing possible alternatives. The water can be obtained from the city, purchased, or gathered from underground wells. This chapter looked into theses water needs and the conditioning that needs to take place so that the water can be used for the electrolysis process.

The geothermal plant was included in the model to create a complete model of the hydrogen production plant. The parameters of the plant were set at values based on current power plants that use geothermal energy as a source for creating electricity. By assuming the geothermal plant operates in a steady state manner, the electrolyzer parameters could be varied in order to determine if there were any efficiency gains or losses in the production of hydrogen. In the combined model the geothermal plant was

connected to the electrolyzer model via a shell and tube heat exchanger. This heat exchanger was designed in order to deliver water at the manufacturer's maximum recommended temperature of 80°C. Based on the results previously discussed, this is the temperature where the electrolyzer is most efficient. This temperature is also dependant on the flow rate from the feed water pump. Once the design of this heat exchanger is set, the flow rate of the pump can be adjusted accordingly. As the demand for hydrogen increases so will the number of the electrolyzers needed to meet the production demands. As this happens the flow rate of the pump can be varied to keep the water temperature before it enters the electrolyzer at a value close to 80°C.

## 6.2 Conclusions

Hydrogen is produced by a number of production methods. In using a renewable energy in geothermal energy the production of hydrogen can be viewed as a carbon free process. The geothermal plant creates the electricity for the electrolysis plant as well as providing energy to the water to reduce the amount of energy required to produce the hydrogen.

The analysis of the water data in Chapter 3 does not meet the water requirements for production electrolyzers. The water from the test sites need to be purified and conditioned considerably in order to be used with the production electrolyzers. This purification can be achieved with modern purification systems to obtain the quality of water required to produce hydrogen efficiently using the methods outlined above.

The data in Chapter 5 show that there are optimal operating characteristics for electrolyzers. The greater the temperature the higher the efficiencies, but there are trade offs with the required amperage. Once a certain value for the current is reached the

overall efficiency begins to drop. Based on the results of the TRNSYS model this current density value is close to 200 $mA/m^2$ or 200 A for the electrolyzer used in this study.

There is a 17% increase in efficiency by increasing the temperature from 20ºC to 80ºC. Increasing the temperature of the electrolyzer will decrease the amount of voltage needed to split water forming hydrogen and oxygen. This decrease amounts to 18% of the cell voltage required when the temperature increases from 20ºC to 80ºC. This decrease in voltage required increases the efficiency of the system.

## 6.3 Recommendations for Future Work

While the nature of the research discussed is focused on the production of hydrogen by the electrolysis, it employs a "big picture" view of the system. There are several areas of the model that can be selected for further research. One of those areas is the electrolyzers. This model takes into consideration the use of one electrolyzer. By increasing the number of electrolyzer to achieve a certain volume of hydrogen over a period of time, one would be able to see the effects this might have on the other system components.

Once the hydrogen is produced, storage and distribution methods need to be considered. Thermal compression of the hydrogen should be investigated as a means to improve system efficiency. This thermal energy could be provided by the geothermal plant as well, thus reducing the amount of energy required for the compression and improve efficiencies. Currently there is not a component within the TRNSYS libraries that model thermal compression. Once a component capable of modeling thermal compression is programmed it can be implemented into the model and the storage of the

hydrogen can be considered. By looking at multiple electrolyzers, thermal compression, and storage possibilities the system could then be optimized more thoroughly.

## References


[1] "Hydrogen, Fuel Cells & Infrastructure Technologies Program, Multi-Year Research, Development and Demonstration Plan", U.S. Department of Energy: Energy Efficiency and Renewable Energy; Hydrogen, Fuel Cells, and Infrastructure Technology Program, Multi-Year Research, Development and Demonstration Plan, February 2005. www.eere.energy.gov/hydrogenandfuelcells/mypp/

[2] "Roadmap on Manufacturing R&D for the Hydrogen Economy," Washington, D.C. [retrieved Dec 2005].

[3] Wertz, D. W., Chemistry A Molecular Science, Prentice Hall, 2002, pp. 245-246.

[4] "$H_2$Fuel the Production, Storage, Distribution, and Use of Hydrogen Fuel by Transit Systems" Prepared for the Regional Transportation Commission of Washoe County, Nevada, Prepared by the University of Nevada, Reno, May 2005.

[5] "TRNSYS 16 a TRaNsient System Simulation program" Vol. 1 pp. 1-7, 2005.

[6] "TRNSYS 16 a TRaNsient System Simulation program" Vol. 3-5 pp. 1-7, 2005.

[7] "T.E.S.S Component Libraries v2.0, for TRNSYS v16.x and the TRNSYS Simulation Studio," Thermal Energy System Specialists, LLC, Nov. 2004.

[8] Schwarzbozl, P., "A TRNSYS Model Library for Solar Thermal Electric Components (STEC) Reference Manual," Nov. 2006.

[9] "Annual Energy Outlook 2006 with Projections to 2030," DOE/EIA-0383, Feb. 2006.

[10] "Natural Gas and the Environment," NaturalGas.org, 2004, http://www.naturalgas.org/environment/naturalgas.asp#greenhouse/ [retrieved May 2006].

[11] "Where Does My Gasoline Come From," Energy Information Administration, Brochure, 2005.

[12] Zittel, W., Ludwig-Bölkow-Systemtechnik, R. W., "Hydrogen in the Energy Sector," Chapter 2, September 1996, http://www.hyweb.de/Knowledge/w-i-energiew-eng2.html, [retrieved Jan. 2007].

[13] Zittel, W., Ludwig-Bölkow-Systemtechnik, R. W., "Hydrogen in the Energy Sector," Chapter 3, September 1996, http://www.hyweb.de/Knowledge/w-i-energiew-eng3.html [retrieved Jan. 2008].

[14] Kruse, B., Grinna, S., Buch, C., "Hydrogen," Bellona rapport nr.6 2002 http://bellona.org/filearchive/fil_Hydrogen_6-2002.pdf [retrieved Jan. 2008].

[15] Crabtree, G. W., Dresselhaus, M. S., and Buchanan, M. V., "The Hydrogen Economy," *Physics Today*, Dec. 2004.

[16] "Hydrogen as an Energy Carrier and its Production by Nuclear Heat," International Atomic Energy Agency (IAEA), IAEA-TECDOC-1085, May 1999.

[17] Çengel, Yunus, A., Boles, Michael, A., Thermodynamics an Engineering Approach, McGraw-Hill, 2002.

[18] Simbeck, D. and Chang, E. "Hydrogen Supply: Cost Estimate for Hydrogen Pathways – Scoping Analysis," NREL/SR-540-32525, Nov. 2002.

[19] "Mineral Commodity Summaries," U.S. Geological Survey, Jan. 2005. http://minerals.usgs.gov/minerals/pubs/commodity/nitrogen/nitromcs05.pdf.

[20] Kreutz, T.G., Williams, R.H., Socolow, P., Chiesa, and G. Lozza., "Production of Hydrogen and Electricity from Coal with $CO_2$ Capture," Proceedings of the 6th International Meeting on Greenhouse Gas Control (GHGT-6), October 1-4, 2002 Kyoto, Japan.

[21] Milne, T. A., Elam, C. C., and Evans, R. J., "Hydrogen from Biomass: State of the Art and Research Challenges," NREL IEA/H2/TR-02/001.

[22] Huang, R., "Hydrogen Production by Photoelectrolysis," http://bhuang02.tripod.com/photoelectrolysis.htm [retrieved Feb. 2008].

[23] "Transport and the Hydrogen Economy," Australian Uranium Association, Briefing paper #73, Jan 2008, http://www.uic.com.au/nip73.htm [retrieved Jan. 2008].

[24] http://www.ne.doe.gov/hydrogen/HTE.pdf [retrieved Nov. 2005].

.

[25] El-Deab, M.S., and Saleh, M.U., "Electrocatalytic production of hydrogen on reticulated vitrous Carbon," *International Journal of Hydrogen Energy*, Nov. 2003, Vol. 28 Issue 11, pp. 1199.

[26] "Hydrogen Produced by High Efficiency Hydrolysis Process," *Advanced Materials & Processes*, Feb. 2005, Vol. 163 Issue 2, pp. 81.

[27] S. A. Grigor'ev, V. I. Porembskii, and V. N. Fateev, "Electrolyzers with Solid Polymer Electrolyte for Getting Special-Purity Gases," *Chemical and Petroleum Engineering*, Vol. 40, Issue 9/10, pp. 606-610.

[28] Farhar, B., and Dunlevy, P., "Feds Identify Opportunites for Potential Geothermal Development on Public Lands," U.S. Department of the Interior, Apr. 2003. http://www.doi.gov/news/030414b.htm.

[29] Wood, B., and Morse, D., "Geothermal Resource Potential within the State of Nevada," $H_2$Fuel Project, Sep. 2005.

[30] "Oversight Hearing: National Energy Policy," Briefing Paper, Committee on Resources, Jun. 2001.

[31] Kutscher, C. F., "The Status and Future of Geothermal Electric Power," National Renewable Energy Laboratory, Jun. 2000.

[32] Renewable Energy Access.com http://www.renewableenergyaccess.com/rea/news/story?id=26591 (comparison of geothermal energy to barrels of oil) [retrieved Apr. 2008].

[33] "Nevada Incentives for Renewable Energy," DSIRE, [retrieved Sep. 2005]. http://www.dsireusa.org/library/includes/map2.cfm?CurrentPageID=1&State=NV.

[34] Gawell, K., "Clean and Diversified Energy Initiative Western Governors' Association," Geothermal Task Force Report, Jan. 2006.

[35] "Testimony of the U.S. Geologic Survey before the Subcommittee on Energy and Mineral Resources of the House Resources Committee," U.S. House of Representatives, May 3, 2001. Note: resource assessments have not been conducted for all states with geothermal potential. *Montana per Dr. John Lund and Washington State estimated by Prof. Gordon Bloomquist.

[36] "Standard Specification for Reagent Water", Designation: D 1193 – 06, An American National Standard, Federal Test Method, Standard No. 7916, 2006.

[37] "$H_2$Fuel the Production, Storage, Distribution, and Use of Hydrogen Fuel by Transit Systems, Part I Summary and Conclusions," University of Nevada, Reno, May 2005.

[38] Ulleberg, O. "Modeling of Advanced Alkaline Electrolyzers: A System Simulation Approach," *International Journal of Hydrogen Energy* 28(10: 7-19), 2002.

[39] Harvie, D. J. E., Davidson, M. R., Rudman, M., "An Analysis of Parasitic Current Generation in Volume of Fluid Simulations," Anziam J. 46(E) pp. C133-C149, 2005.

[40] Elam, C., Kroposki, B., Bianchi, G., Harrison, K., "Renewable Electrolysis Integrated System Development and Testing," National Renewable Energy Laboratory, II.F.2, 2004.

[41] KPRO, Programm zur Berechnung von Kreisprozessen (Simulation Code for the Evaluation of Power Cycles), Vers. 4.1 Fichtner, Stuttgart, 1997.

[42] Zemke, P.E., and Wood, B.D., "Hybrid Solar Lighting May Have Another Utility: Solar Water Heating," *Solar Engineering*, 2006, pp. 365-370.

[43] Solar Rating and Certification Corporation. SRCC Document G-300, Operating Guideline and Minimum Standards for Certifying Solar Water Heating Systems, 2002.

[44] Duncan, C., Ormat, telephonic conversation, Jun. 2006.

# Appendices

# Appendix A TRaNsient SyStem Simulation program

## A.1 Introduction

Today computer modeling is being used in an increasing number of applications in the engineering field as well as other fields. These modeling programs reduce testing procedures and the overall design process. Experiments are still necessary to validate the programs results, but you are able to predict with increasing certainty the results of the experiments. These modeling programs allow an engineer to visualize, conceptualize, and even predict certain outcomes based in the inputs of a project. Although the modeling programs can not create real world situations with perfection, they're accuracy is improving as computer programmers become more knowledgeable and skilled.

## A.2 Objective

The objective of this project is to become familiar with TRNSYS and use this knowledge to develop a simple solar water heating model. This model will then be compared against *F-Chart* results [3] as well as industry standards set forth by the Solar Rating & Certification Corporation [2] to determine the accuracy of the program and the modeling techniques employed by the programmer.

## A.3 Theory

TRNSYS is a simulation environment for the transient simulation of energy systems. It is used to validate new energy concepts, design these or other concepts, their equipment, control strategies, occupant behavior, alternative energy systems, etc. It has an open, modular structure that allows the user to access the source code and manipulate that code as the user see fit [1]. In this project said program will be used determine the model characteristics as defined above.

## A.4 Method

The solar water heating system to be modeled can be found in Fig A.1.

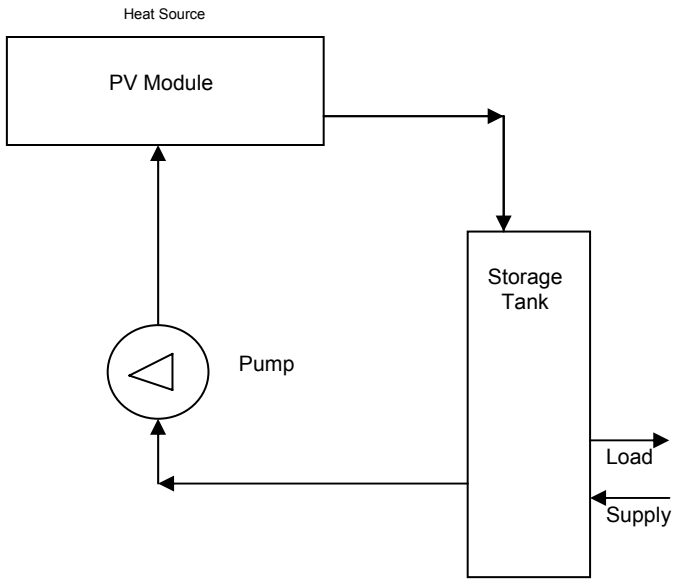


Fig. A.1: Sketch of solar water heating system.

An understanding of the system is necessary to model the system in TRNSYS. First global parameters are defined. The global criterions for this system are the fluid, location, and time of simulation. The location of the system is Phoenix, AZ, water is the fluid and the month of interest is July. TRNSYS employees components that are already programmed within the modeling package and are ready to be used. The necessary components for this model are listed in Table A.1.

Table A.1: List of System Components

| Component | Description |
|---|---|
| Type 1b | Solar Collector; flat plate, Quadratic Efficiency, 2nd Order Incidence Angle Modifiers |
| Type 3b | Pump |
| Type 4a | Storage Tank; Fixed Inlets, Uniform Losses |
| Type 109 TMY2 | Weather Data Reader and Radiation Processor |
| Type 14h | Time Dependent Forcing Function |
| Type 682 | Heating and Cooling Loads Imposed on a Flow Stream |
| Type 24 | Quantity Integrator |
| Type 65d | Online graphical plotter |

After the components have been selected, the necessary connections are made and the parameters for various components are adjusted to the desired values. The online printers are then used to display the results.

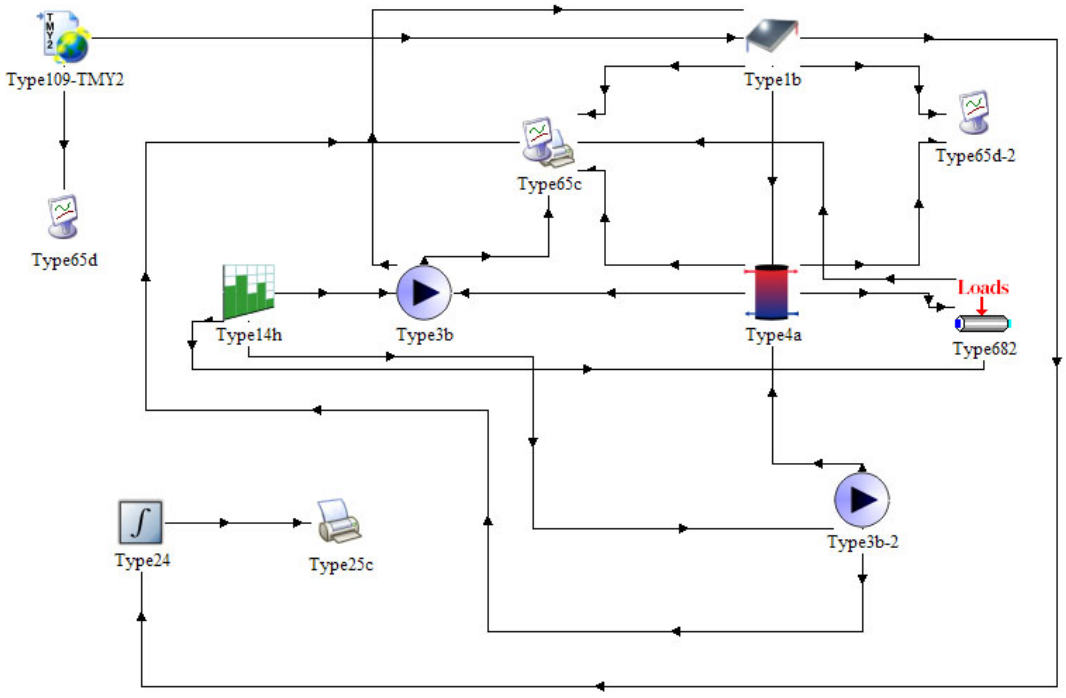


Fig. A.2: TRNSYS solar water heating model.

## A.5 Results

The program was simulated for the month of July as well as a chosen day in July. The results are found in the following charts produced by TRNSYS' online plotter. The load and pumps are a constant for each day in the simulation that runs for a month. In the simulation that runs for a day the load and pumps are turned on at 8am and then turned off at 4:30pm to better simulate water usage during the day.

Fig. A.3-A.8 display the results for the one month simulation time

Fig. A.9-A.16 display the results for the one day simulation time

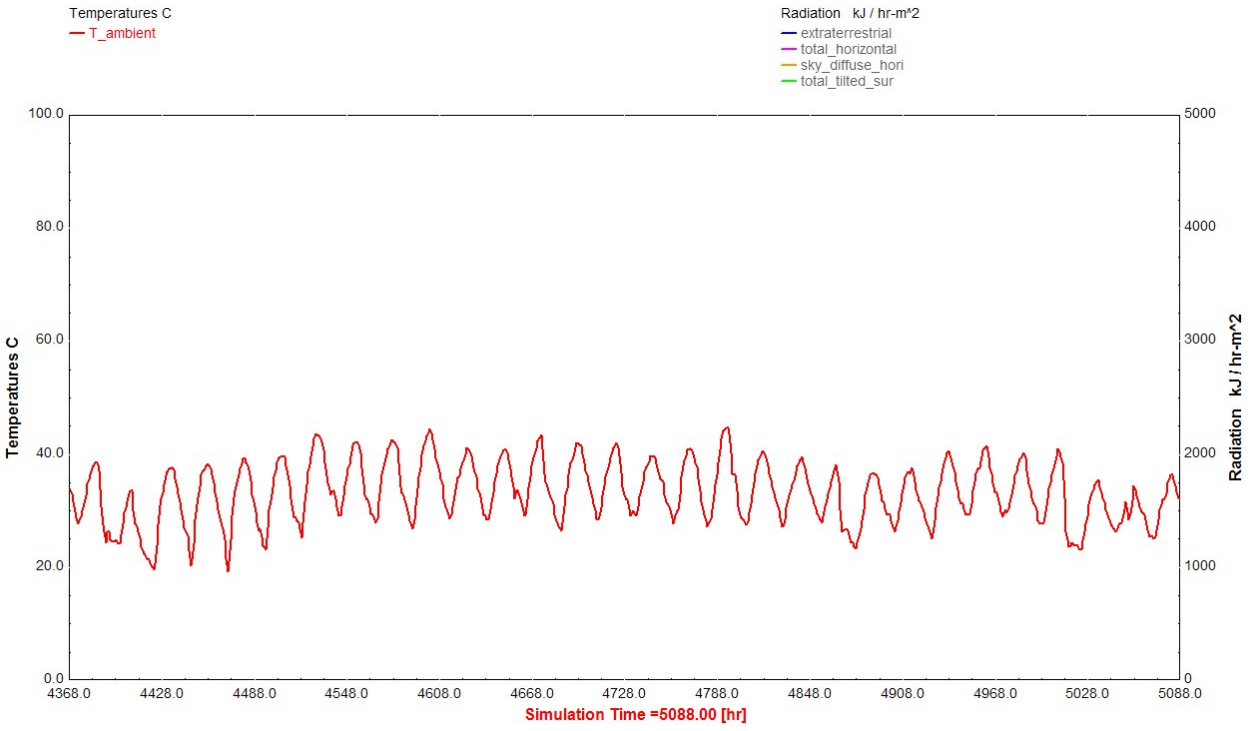


Fig. A.3: Ambient temperature for the month of July in Phoenix, AZ using TMY data.

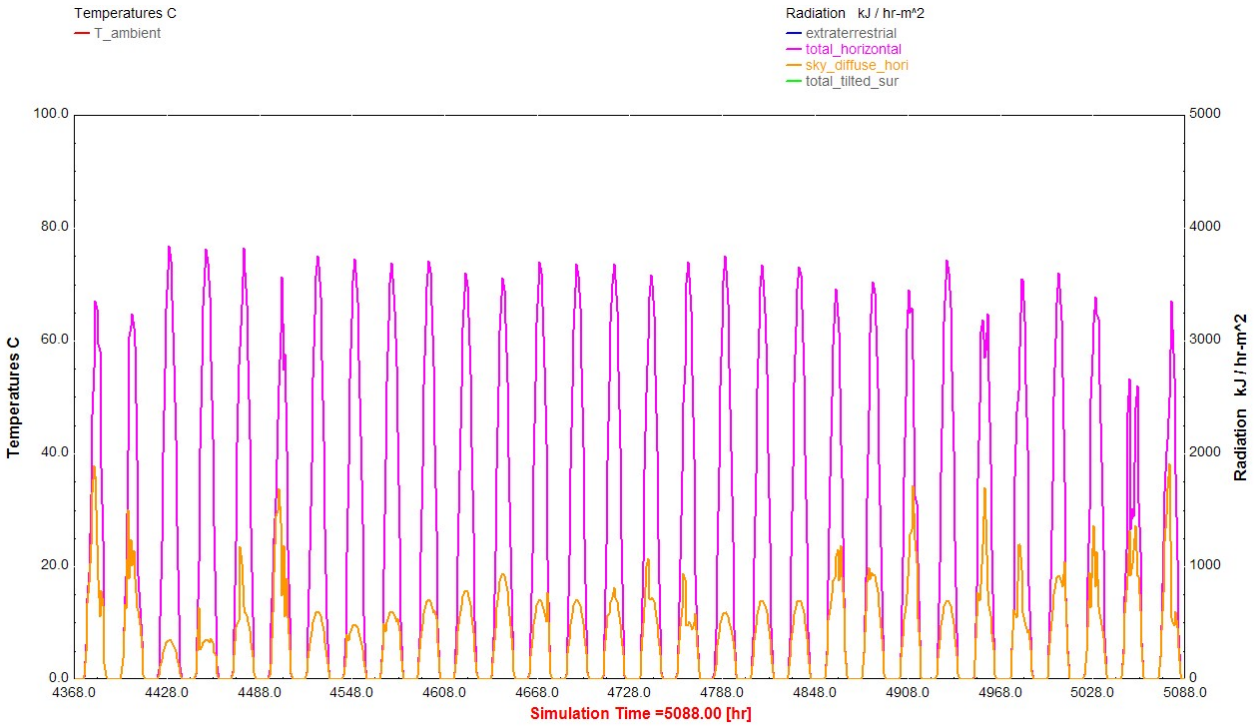


Fig. A.4: Total horizontal and sky diffuse horizontal radiation for the month of July.

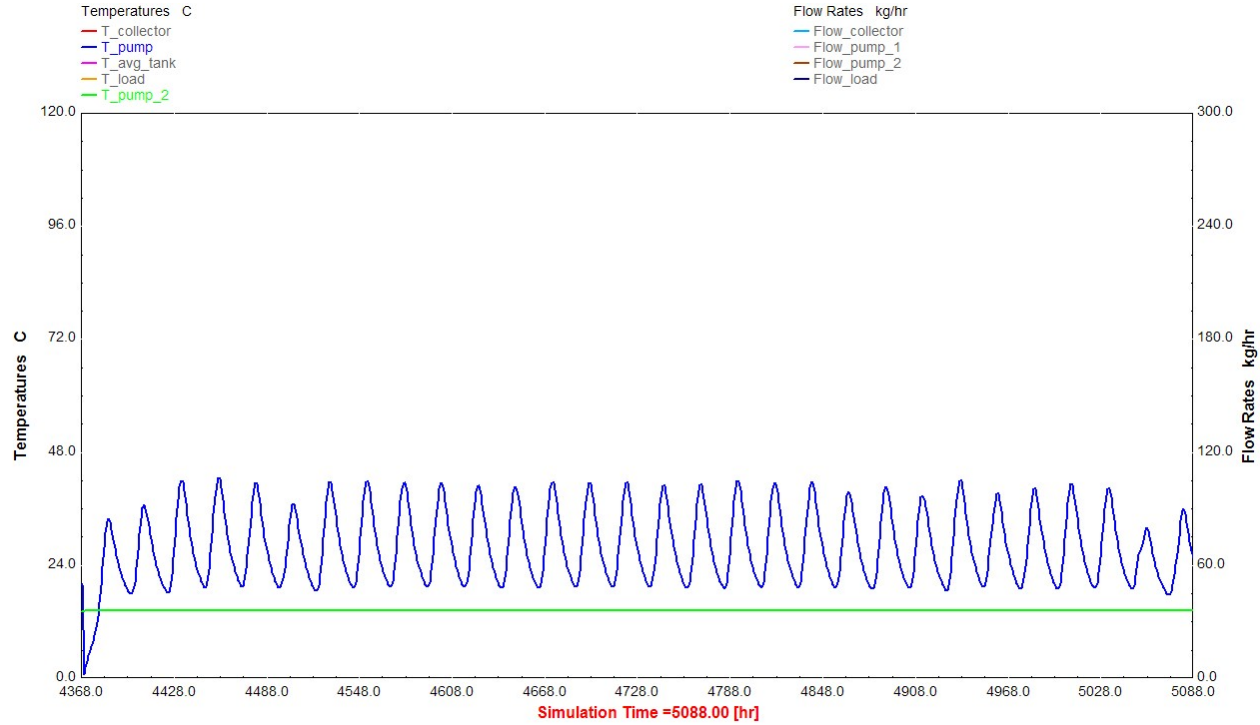


Fig. A.5: Temperature of pump 1 and pump 2 (water supply).

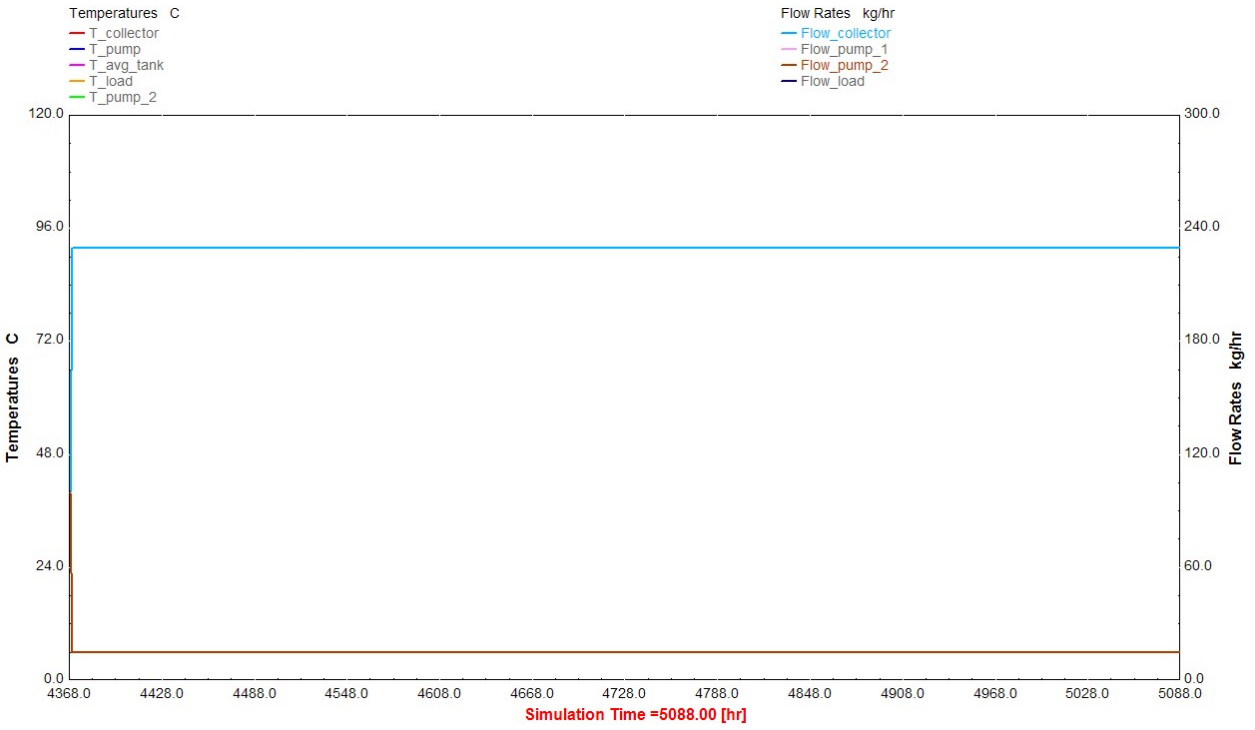


Fig. A.6: Flow rates through the collector and the supply pump.

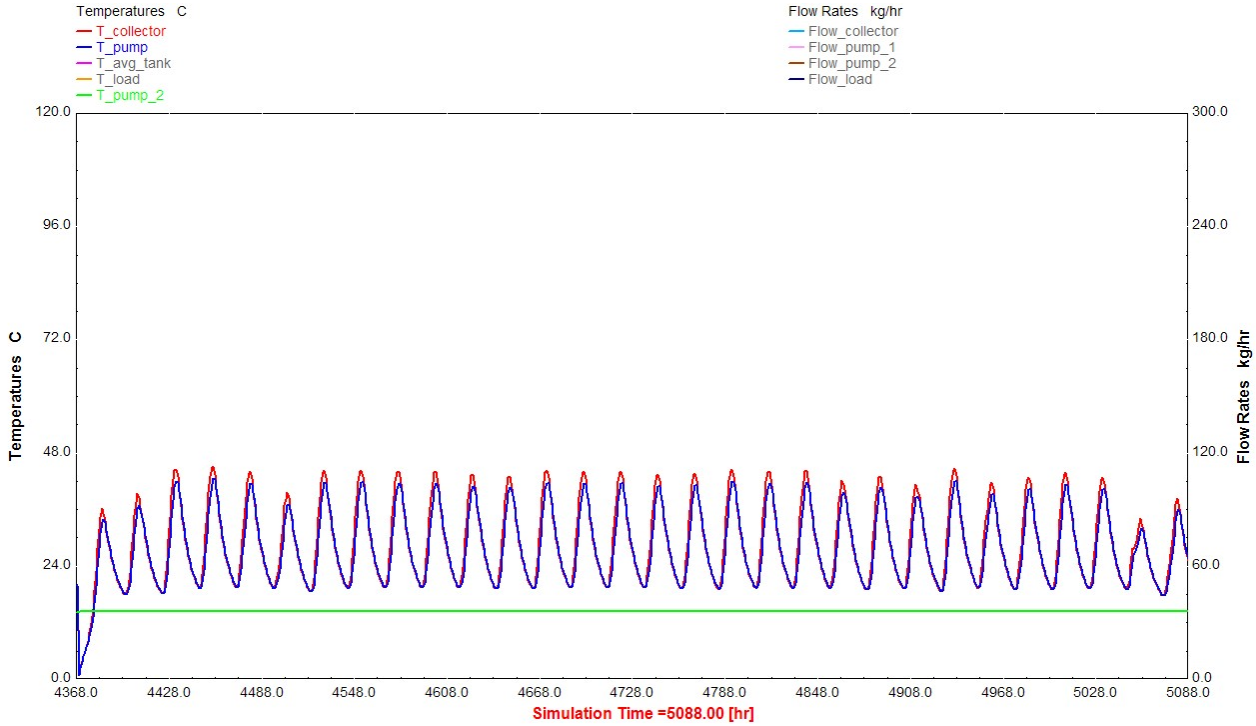


Fig. A.7: Temperatures of the collector, tank, and supply.

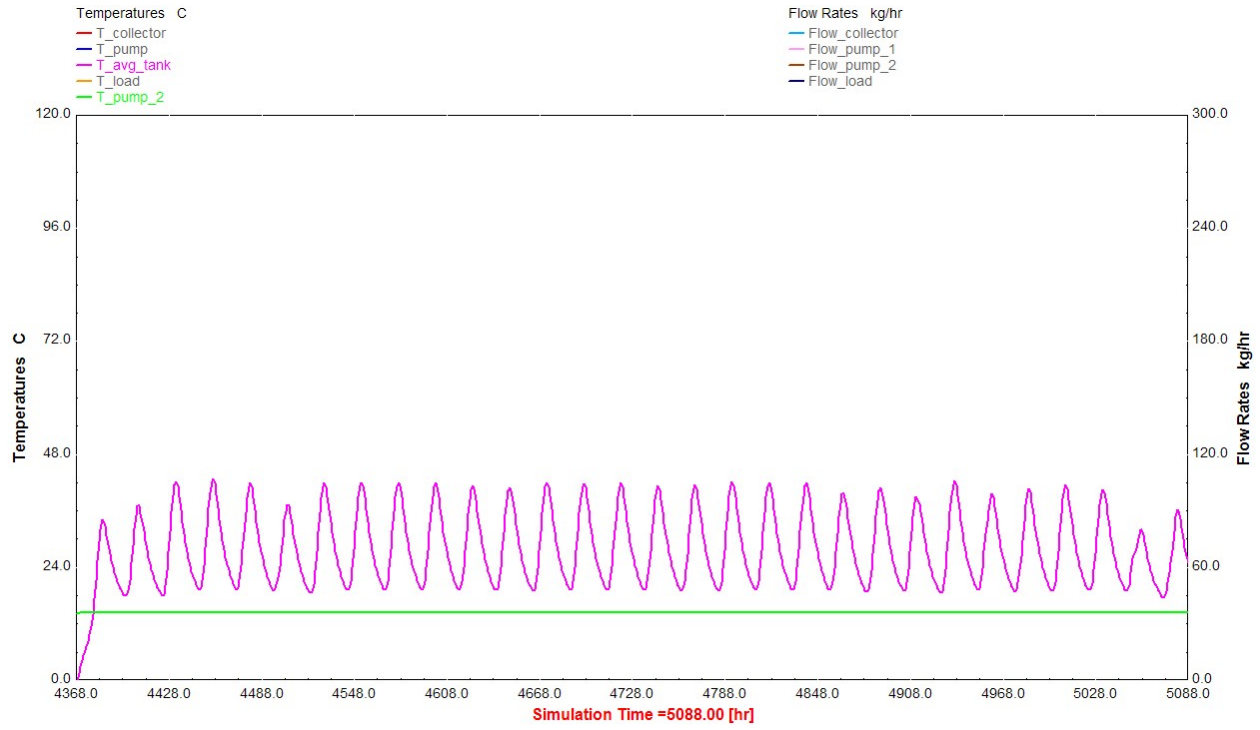


Fig. A.8: Temperature of the tank compared to the supply.

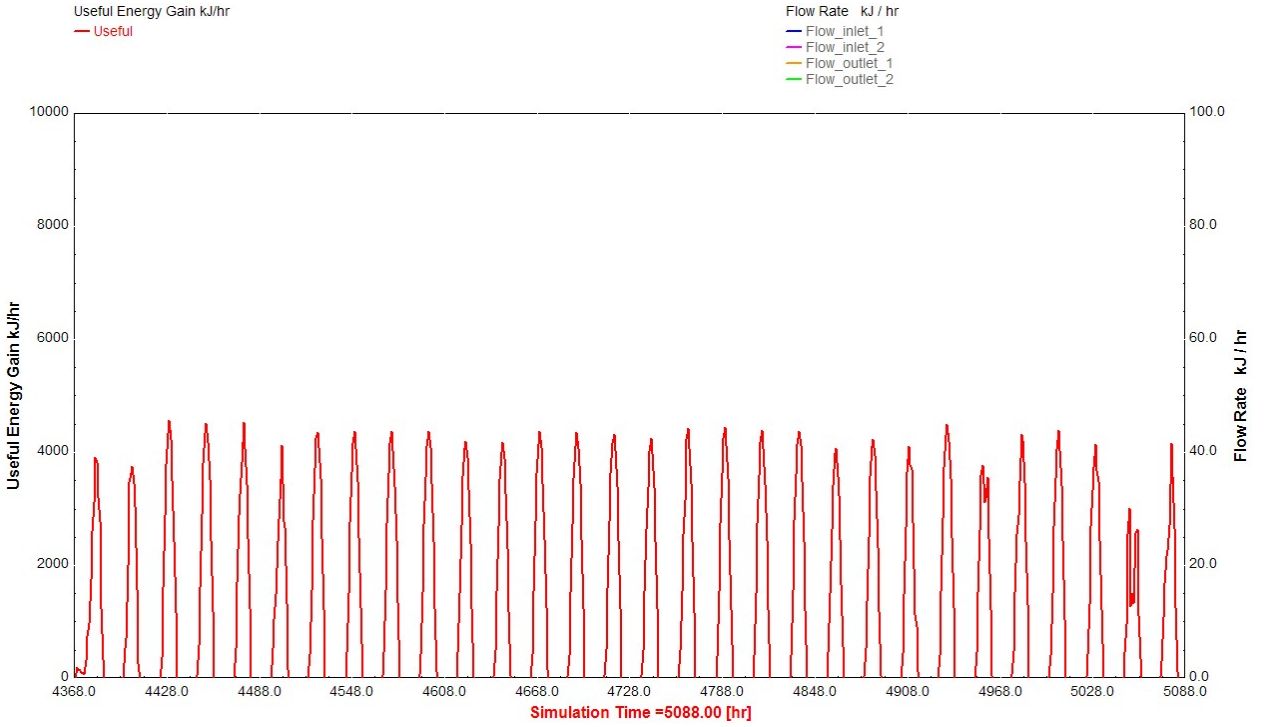


Fig. A.9: Useful energy gain of the system [ kJ / hr ].

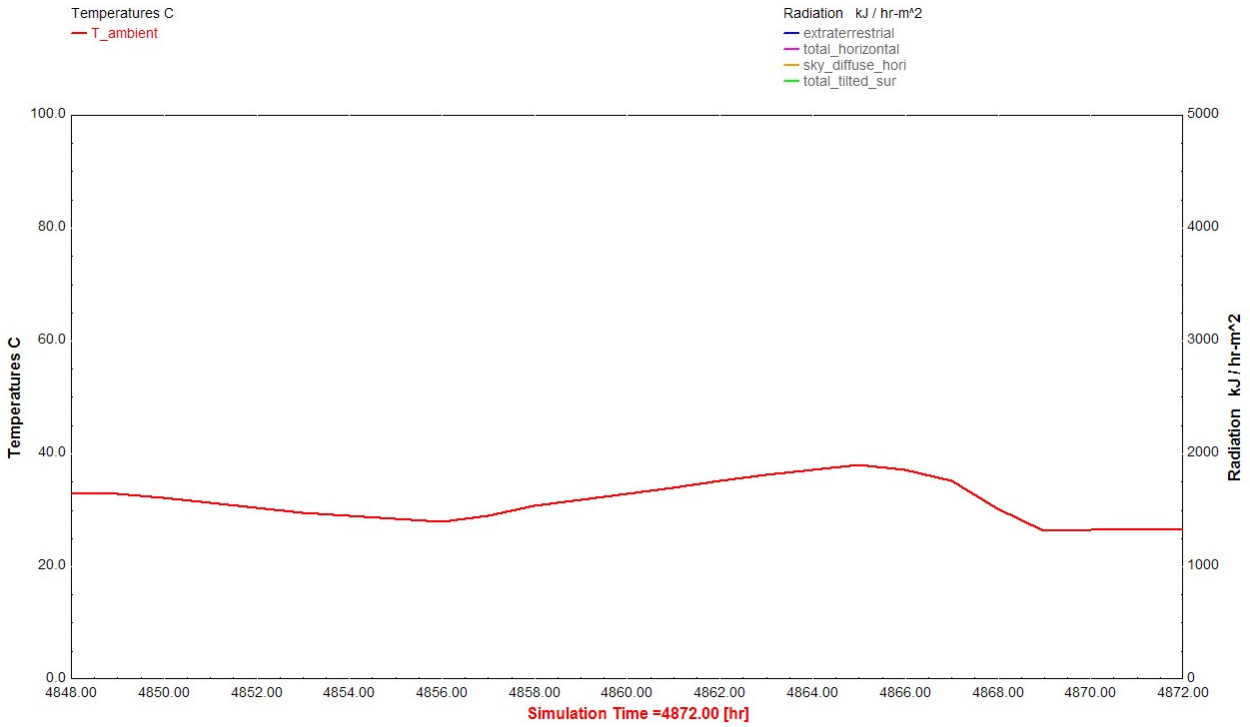


Fig. A.10: Ambient temperature July 21, Phoenix, AZ using TMY data.

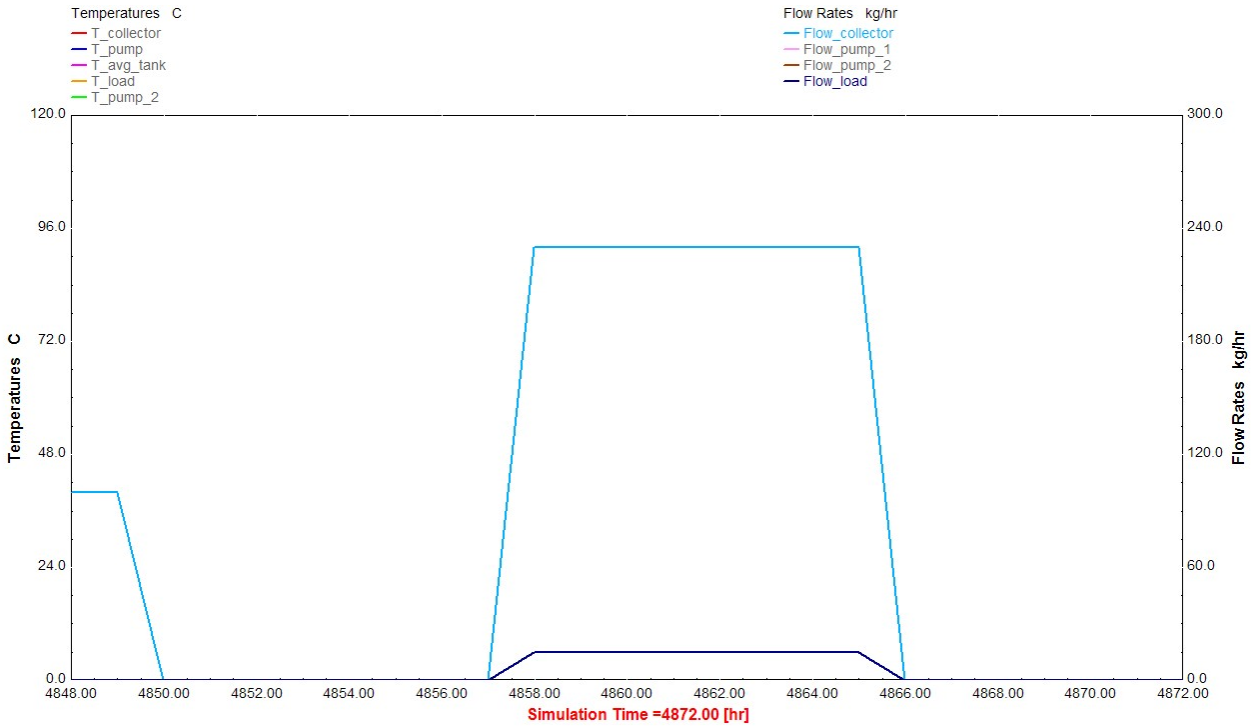


Fig. A.11: Flow through the collector vs. the supply flow rate.

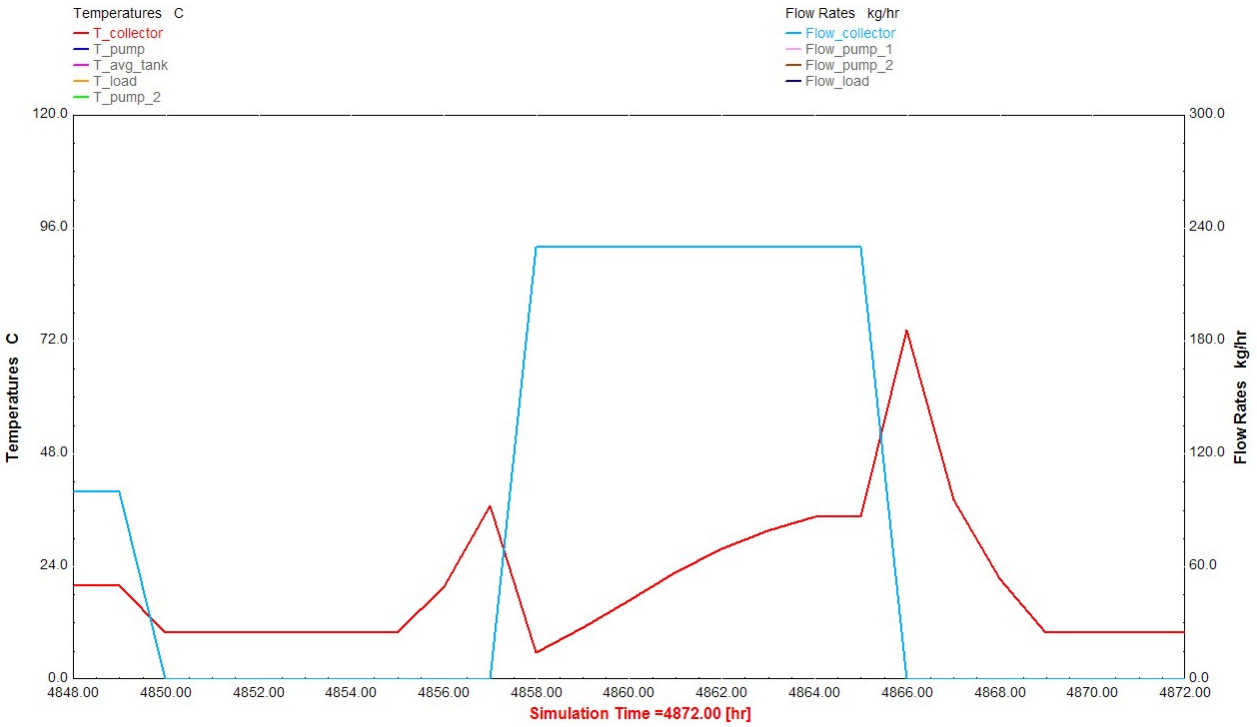


Fig. A.12: Temperature of the collector vs. the flow rate through the collector.

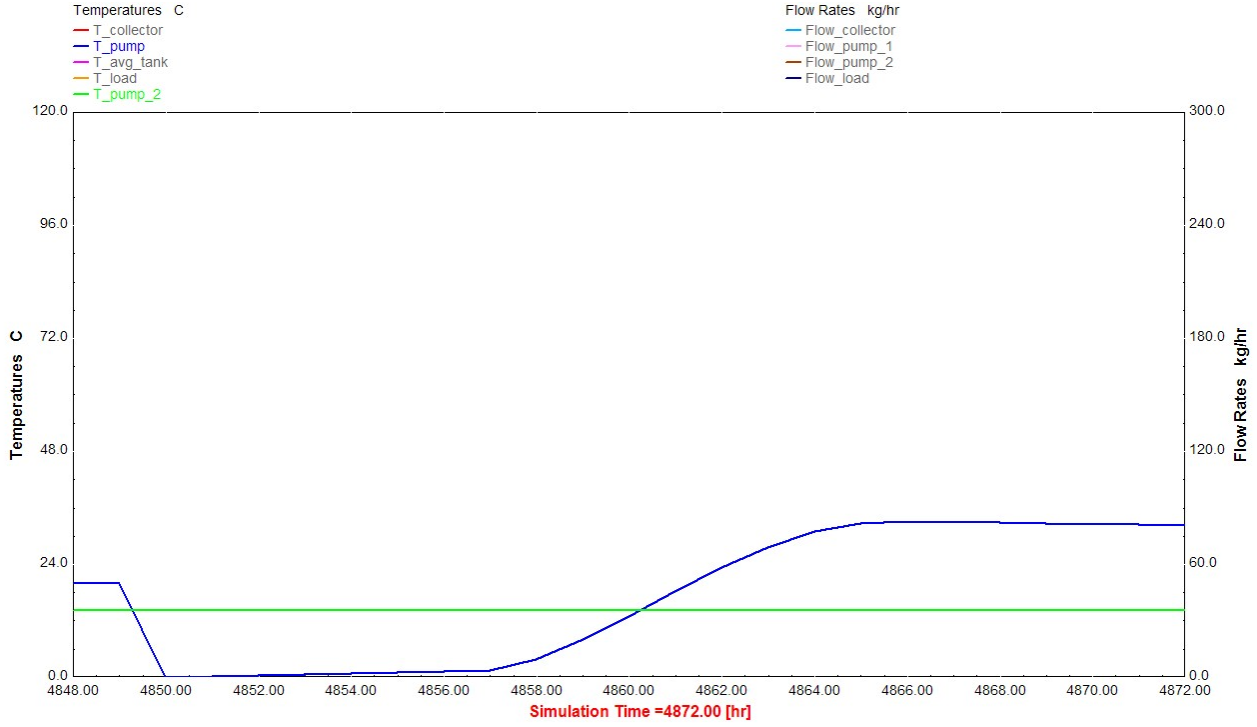


Fig. A.13: Temperature of through pump 1 vs. the supply temperature.

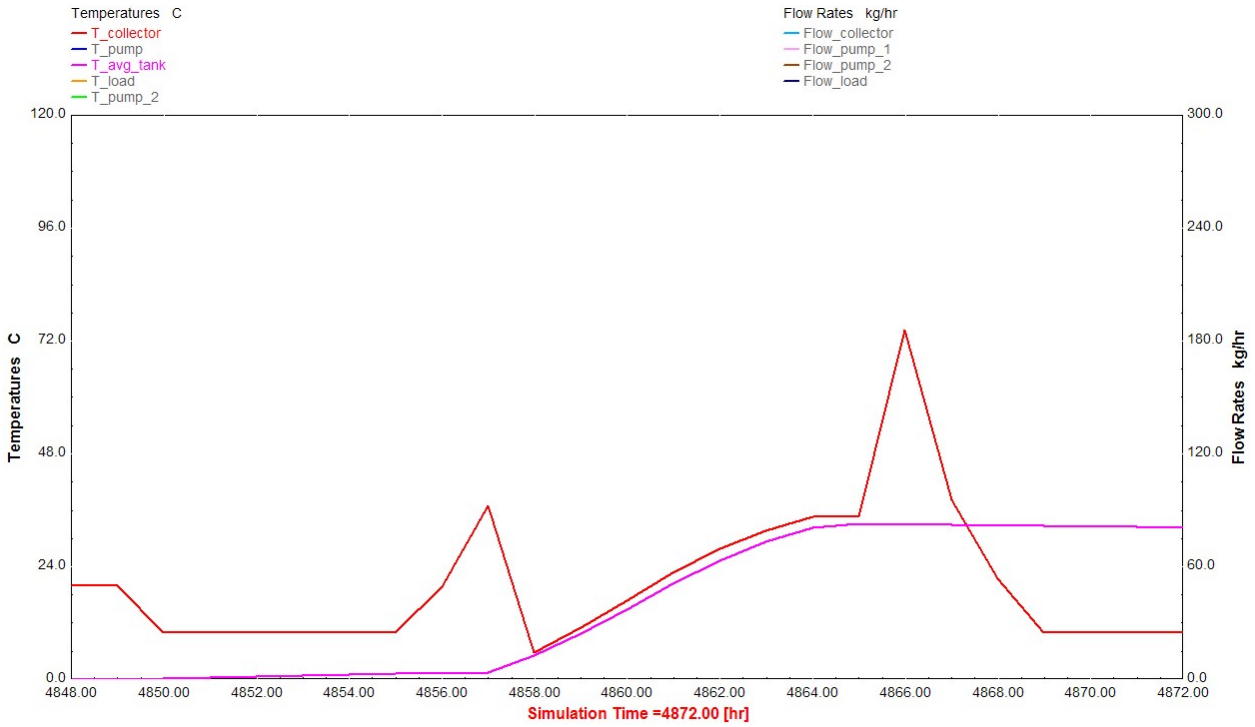


Fig. A.14: Temperature of the collector vs. the average tank temperature.

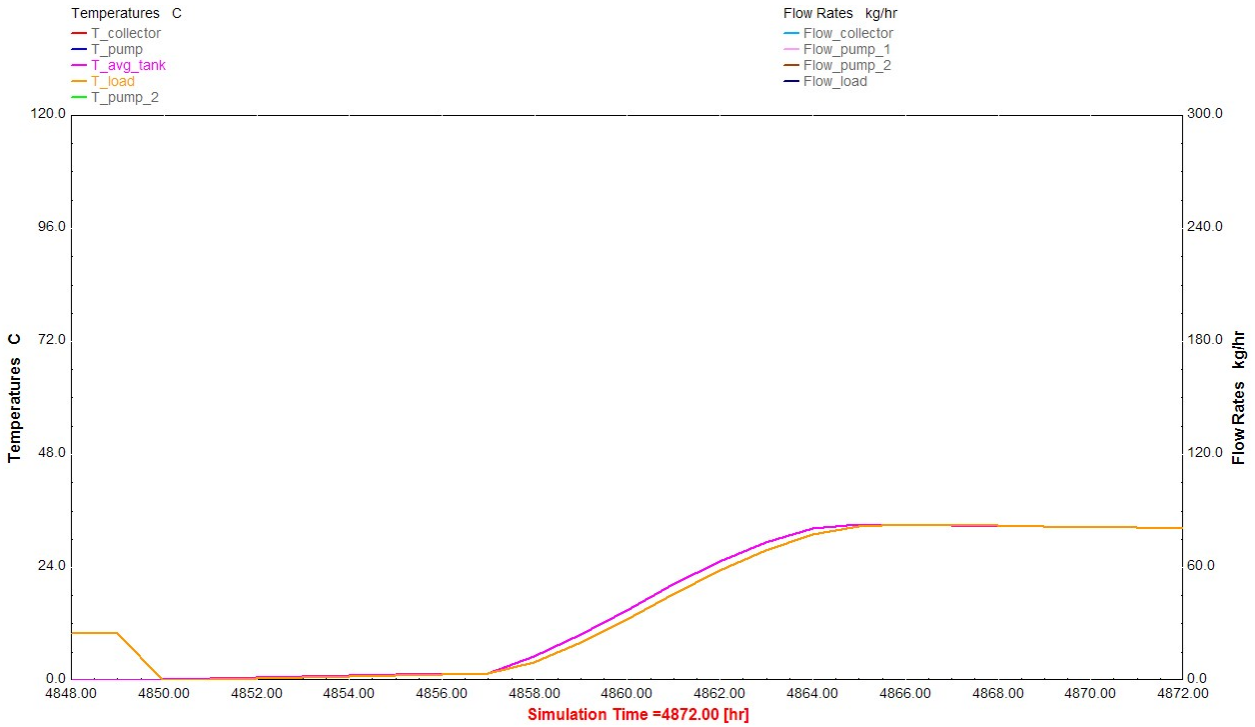


Fig. A.15: Temperature of the load vs. the average temperature of the tank.

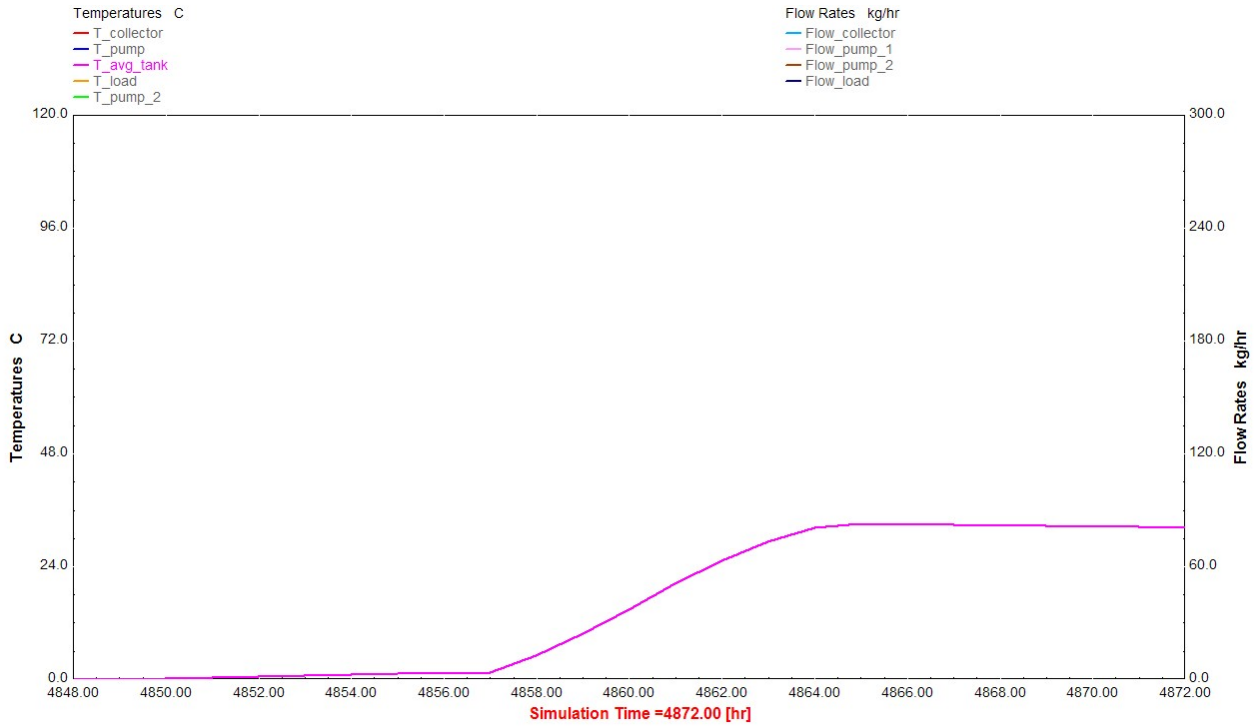


Fig. A.16: Average tank temperature.

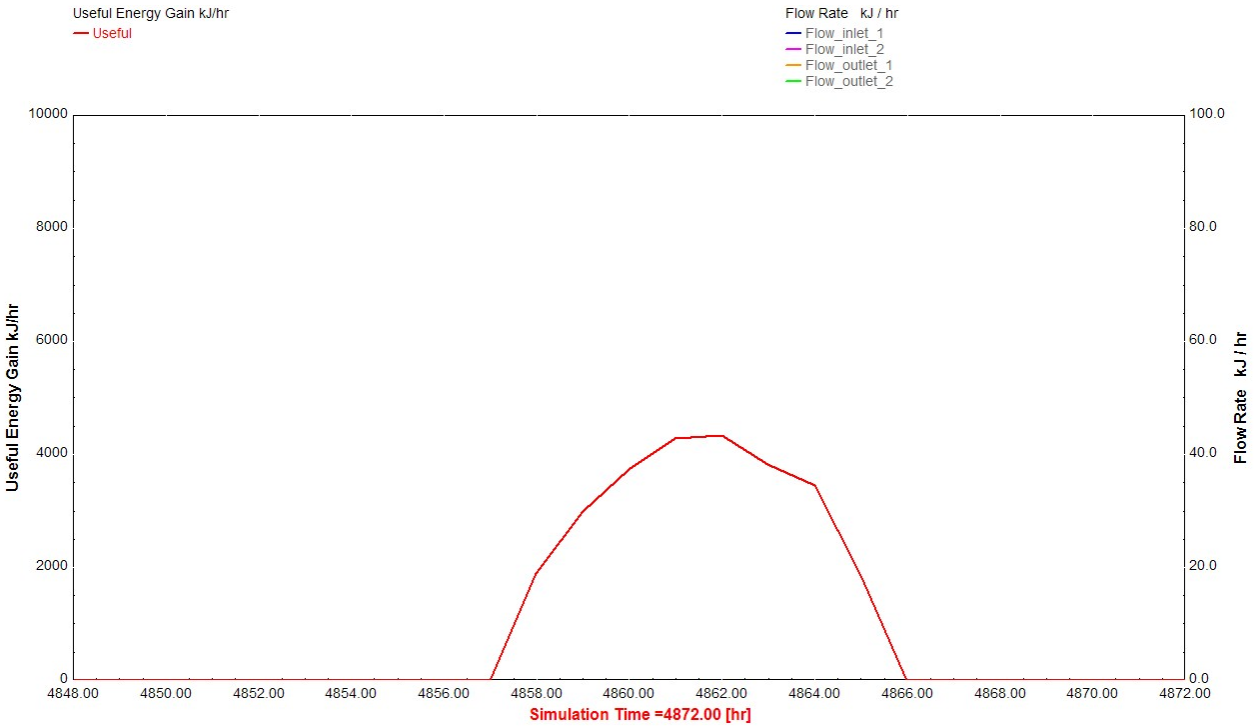


Fig. A.17: Useful energy gain of the system [ kJ / hr ].

## A.6 Discussion of Results

In order to compare the TRNSYS model with the SRCC standards and the F-chart results some kind of uniformity needs to be taken into consideration. The SRCC uses a solar energy factor (SEF) to compare current models that are manufactured. The SRCC also uses certain parameters used by the U.S. Department of Energy to test for water heaters. The current TRNSYS model uses these initial parameters as well as the F-chart results [3]. The SEF value is calculated using the following formula [2]:

$$SEF = \frac{Q_{DEL}}{Q_{AUX} + Q_{PAR}}.$$

$Q_{DEL}$ = Energy delivered to the hot water load.

$Q_{AUX}$ = Daily amount of energy used by the auxiliary water heater or backup element with a solar system operating.

$Q_{PAR}$ = Parasitic energy: Daily amounts of AC electrical energy used to power pumps, controllers, shutters, trackers, or any other item needed to operate the system.

The SEF value of the TRNSYS model for the one day simulation is 2.75. An SRCC certified system with the same configuration has an SEF value of 1.4. The reason for the difference can be explained in the equation. $Q_{DEL}$ is dependant on the energy of the hot water load. This value is as factor of the change in temperature. The TRNSYS model is simulated during on of the hottest times of the year in the desert. This creates a larger change in temperature creating a larger SEF. The SRCC takes an average day of the year, where the temperature difference is not as large, to compute their SEF value. This difference creates discrepancy in the SEF values. A SEF value of 2.75 can be justified by the larger temperature difference in the data used by the simulation.

## A.7 Conclusion

TRNSYS has the capability of model systems to help designers understand a system without experimenting. The results from this exercise show that TRNSYS can produce accurate results that are comparable with industry standards and other programs.

## A.7 References

1. 2005 “TRNSYS 16 a TRaNsient System Simulation program” Vol. 1 pp. 1-7

2. Solar Rating and Certification Corporation. 2002. SRCC Document )G-300. Operating Guideline and Minimum Standards for Certifying Solar Water Heating Systems.

3. Zemke, P.E., and Wood, B.D.,2006, “Hybrid Solar Lighting May Have Another Utility: Solar Water Heating”, pp. 1-5

# Appendix B Complete TRNSYS Electrolyzer Model Equations

## B.1 Electrochemical Model

Resistance in electrolyte

$$r` = r_1 + r_2 \cdot T_{ely} \quad A1$$

Overvoltages on electrodes

$$s` = s_1 + s_2 \cdot T_{ely} + s_3 \cdot T_{ely}^{2} \quad A2$$

$$t` = t_1 + \frac{t_2}{T_{ely}} + \frac{t_3}{T_{ely}^{2}} \quad A3$$

Current density

$$I_{density} = \frac{I_{ely}}{AREA \cdot 10} \quad A4$$

Overall efficiency

$$\eta_{tot} = \eta_e \cdot \eta_f$$

Production flow rates (standard cubic meters)

$$\dot{V}_{H2} = \frac{\dot{n}_{H2}}{\rho_{STD}} \cdot 3600$$

$$\dot{V}_{C2} = \frac{\dot{n}_{C2}}{\rho_{STD}} \cdot 3600$$

Density of gas at standard conditions

$$\rho_{STD} = P_{std} \cdot \frac{100000}{RGAS \cdot (TSTD + 273.15)}$$

Stack voltage

$$U_{ely} = N_{cells} \cdot U_{cell}$$

Stack power

$$P_{tot} = U_{ely} \cdot I_{ely} \quad A5$$

## B.2 Thermodynamic Model

Temperatures

$$T_{ely}' = \text{ConvertTemp}(C, K, T_{ely}) \quad A6$$

$$T_{H2} = T_{ely}$$

$$T_{O2} = T_{ely}$$

$$T_{H2O} = T_{ely}$$

Enthalpy

$$\Delta H_{H2} = C_{p0,H2} \cdot (T_{H2} - TREF) + \Delta H0F_{H2}$$

$$\Delta H_{O2} = C_{p0,O2} \cdot (T_{O2} - TREF) + \Delta H0F_{O2}$$

$$\Delta H_{H2O} = C_{p0,H2O} \cdot (T_{H2O} - TREF) + \Delta H0F_{H2O}$$

$$\Delta H = \Delta H_{H2} + 0.5 \cdot \Delta H_{O2} - \Delta H_{H2O} \quad A7$$

Entropy

$$S_{H2} = C_{p0,H2} \cdot \ln\left[\frac{T_{H2} + 273.15}{TREF + 273.15}\right] - RGAS \cdot \ln\left[\frac{P_{ely}}{PREF}\right] + S0F_{H2}$$

$$S_{O2} = C_{p0,O2} \cdot \ln\left[\frac{T_{O2} + 273.15}{TREF + 273.15}\right] - RGAS \cdot \ln\left[\frac{P_{ely}}{PREF}\right] + S0F_{O2}$$

$$S_{H2O} = C_{p0,H2O} \cdot \ln\left[\frac{T_{H2O} + 273.15}{TREF + 273.15}\right] + S0F_{H2O}$$

$$\Delta S = S_{H2} + 0.5 \cdot S_{O2} - S_{H2O} \quad A8$$

## B.3 Thermal Model

Thermal capacitance

$$C_T = \tau_T \cdot \frac{3600}{R_T} \quad \text{A9}$$

Heat capacityof cooling water

$$C_{p,H2O} = V_{cw} \cdot \frac{\rho_{H2O}}{M_{H2O}} \cdot C_{p0,H2O} \cdot \frac{1000}{3600} \quad \text{A10}$$

Overall UAfor cooling water heat exchanger

$$UA_{HX} = h_1 + h_2 \cdot I_{ely}$$

Cooling water outlet temperature

$$T_{cw,out} = T_{cw,in} + (T_{ely} - T_{cw,in}) \cdot \left[1 - \exp\left(\frac{-UA_{HX}}{C_{p,H2O}}\right)\right] \quad \text{A11}$$

Analytically solving the differential equiation

$$T_{ely} = T_{ini} + \int_0^{DELT} (dTdt_{ely})\ d\,Time \quad \text{A12}$$

The TYPE 160 solves the equation analytically.

## B.4 Operational Characteristics

Parameters

AREA = **Lookup** ( 'Parameter', 1, 'Value' )

$N_{cells}$ = **Lookup** ( 'Parameter', 2, 'Value' )

$R_T$ = **Lookup** ( 'Parameter', 3, 'Value' )

$\tau_T$ = **Lookup** ( 'Parameter', 4, 'Value' )

$r_1$ = **Lookup** ( 'Parameter', 5, 'Value' )

$r_2$ = **Lookup** ( 'Parameter', 6, 'Value' )

$s_1$ = **Lookup** ( 'Parameter', 7, 'Value' )

$s_2$ = **Lookup** ( 'Parameter', 8, 'Value' )

$s_3$ = **Lookup** ( 'Parameter', 9, 'Value' )

$t_1$ = **Lookup** ( 'Parameter', 10, 'Value' )

$t_2$ = **Lookup** ( 'Parameter', 11, 'Value' )

$t_3$ = **Lookup** ( 'Parameter', 12, 'Value' )

$a_1$ = **Lookup** ( 'Parameter', 13, 'Value' )

$a_2$ = **Lookup** ( 'Parameter', 14, 'Value' )

$h_1$ = **Lookup** ( 'Parameter', 15, 'Value' )

$h_2$ = **Lookup** ( 'Parameter', 16, 'Value' )

## B.5 Constants

$TSTD = 0$

$P_{std} = 1$

$TREF = 25$

$PREF = 1$

$F = 96485$

$RGAS = 8.3145$

$n = 2$

$M_{H2O} = 18.016$

$\rho_{H2O} = 1000$

$\Delta HOF_{H2O} = -286000 \quad \Delta HOF_{H2} = 0 \quad \Delta HOF_{O2} = 0$

$SOF_{H2O} = 70 \quad SOF_{H2} = 131 \quad SOF_{O2} = 205$

$C_{p0,H2O} = 75 \quad C_{p0,H2} = 29 \quad C_{p0,O2} = 29$

## B.6 Inputs

$DELT = 60$

$w = 10$

$T_{ini} = \textbf{Lookup}$ ( 'Test of iteration', w , 'Tini' )

$P_{ely} = 7$

$I_{ely} = 500$

$T_{amb} = 20$

$T_{cw,in} = 14.5$

$V_{cw} = 0.58$